Forsmark site investigation

Borehole KFM01A

Uniaxial compression test of intact rock

Lars Jacobsson

SP Swedish National Testing and Research Institute

December 2004

SKB

Forsmark site investigation

Borehole KFM01A

Uniaxial compression test of intact rock

Lars Jacobsson

SP Swedish National Testing and Research Institute

December 2004

This report concerns a study which was conducted for SKB. The conclusions and viewpoints presented in the report are those of the author and do not necessarily coincide with those of the client.

A pdf version of this document can be downloaded from www.skb.se

Abstract

Uniaxial compression tests, containing the complete loading response beyond compressive failure, so called post-failure tests, were carried out on 15 water saturated specimens of intact rock from borehole KFM01A in Forsmark. The cylindrical specimens were taken from drill cores at three depth levels ranging between 225–230 m, 496–498 m and 690–691 m. Moreover, the rock type was medium-grained metagranite (-granodiorite). The wet density of the specimens was determined before the mechanical tests, from which the elastic properties, represented by Young's modulus and the Poisson ratio, and the uniaxial compressive strength were deduced. The specimens were photographed before and after the mechanical testing.

The measured densities of the water saturated specimens were in the range 2,650–2,660 kg/m^3 and had a mean value of 2,657 kg/m^3 and the peak values of the axial compressive stress were in the range 187.4–288.6 MPa with a mean value of 239.2 MPa. The elastic parameters were determined at a load corresponding to 50% of the failure load. It was found that Young's modulus was in the range 74.0–81.9 GPa with a mean value of 77.4 GPa, whereas the Poisson ratio was in the range of 0.14–0.28 with a mean value of 0.22. It was seen from the mechanical tests that the material in the specimens responded in a brittle way.

Contents

5

1   Introduction

Uniaxial compression tests, with loading beyond the failure point into the post-failure regime, have been conducted on water-saturated specimens sampled from borehole KFM01A in Forsmark, see map in Figure 1-1. These tests belong to one of the activities performed as part of the site investigation in the Forsmark area managed by the Swedish Nuclear Fuel and Waste Management Co (SKB). The tests were carried out in the material and rock mechanics laboratories at the department of Building Technology and Mechanics at the Swedish National Testing and Research Institute (SP). All work was carried out in accordance with the activity plan AP PF 400-03-18 (SKB internal controlling document) and was controlled by SP-QD 13.1 (SP internal quality document).

SKB supplied SP with rock cores and they arrived at SP in February 2003 and were tested during June 2004. Cylindrical specimens were cut from the cores and selected based on the preliminary core logging with the strategy to primarily investigate the properties of the dominant rock types. The method description SKB MD 190.001, version 1.9 (SKB internal controlling document), was followed for the sampling and for the uniaxial compression tests, and the method description SKB MD 160.002, version 1.9 (SKB internal controlling document), was followed when the density was determined. As to the specimen preparation,
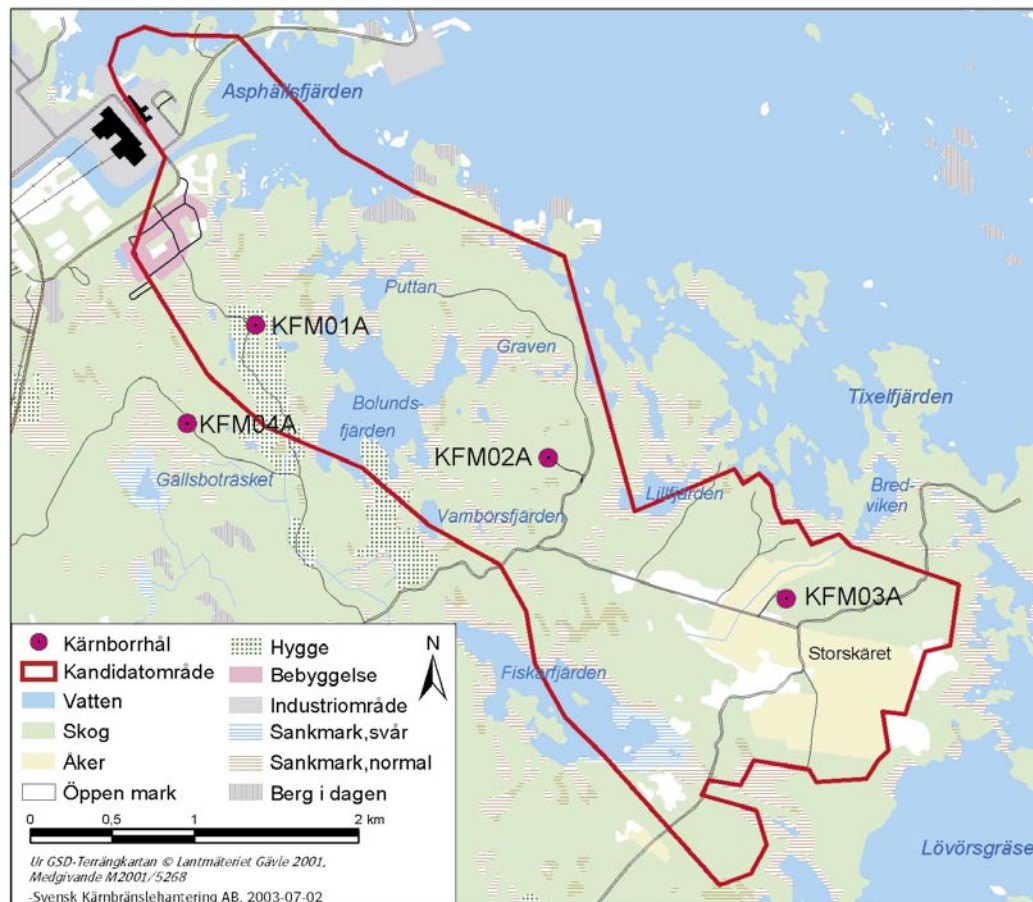

Figure 1-1. *Location of borehole KFM01A at the Forsmark site.*

the end surfaces of the specimens were grinded in order to comply with the required shape tolerances and the specimens were then stored in water, for a minimum of 7 days, up to testing. This yields a water saturation, which is intended to resemble the in-situ moisture condition. The density was determined on each specimen and the uniaxial compression tests were carried out at this moisture condition. The specimens were photographed before and after the mechanical testing.

The uniaxial compression tests were carried out using radial strain as the feed back signal in order to obtain the complete response in the post-failure regime on brittle specimens as is described in the method description SKB MD 190.001, version 1.9, and in the ISRM suggested method /1/. The axial ε_a and radial strain ε_r together with the axial stress σ_a were recorded during the test. The peak value of the axial compressive stress σ_c was determined at each test. Furthermore, two elasticity parameters, Young's modulus E and Poisson ratio v, were deduced from the tangent properties at 50% of the peak load. Diagrams with the volumetric and crack volumetric strain versus axial stress are reported. These diagrams can be used to determine crack initiation stress σ_i and the crack damage stress σ_d, cf /2, 3/.

2   Objective and scope

The purpose of the testing is to determine the uniaxial compressive strength and the elastic properties, represented by Young's modulus and the Poisson ratio, of cylindrical specimens of intact rock sampled from drill cores. Moreover, the specimens have a water content corresponding to the in-situ conditions. The loading is carried out into the post-failure regime in order to study the mechanical behaviour of the rock after cracking, thereby enabling determination of brittleness and residual strength. The specimens originate from borehole KFM01A, which is a near-vertical telescopic borehole of SKB-chemistry type with a drilling length of c 1,000 m.

The results from the tests are to be used in the site descriptive rock mechanics model, which will be established for the candidate area selected for site investigations at Forsmark.

3 Equipment

3.1 Specimen preparation and density measurement

A circular saw with a diamond blade was used to cut the specimens to their final lengths. The surfaces were then grinded after cutting in a grinding machine in order to achieve a high-quality surface for the axial loading that complies with the required tolerances. The measurements of the specimen dimensions were made with a sliding calliper. Furthermore, the tolerances were checked by means of a dial indicator and a stone face plate. The specimen preparation was carried out in accordance with ASTM 4543-01 /4/.

The specimens and the water were weighed using a scale weighing machine.
A thermometer was used for the water temperature measurement. The calculated wet density was determined with an uncertainty of ± 4 kg/m^3.

3.2 Mechanical testing

The mechanical tests were carried out in a servo controlled testing machine specially designed for rock tests, see Figure 3-1. The system consists of a load frame, a hydraulic pump unit, a controller unit and various sensors. Communication with the controller unit

Figure 3-1. *Rock testing system. From left: Digital controller unit, pressure cabinet (used for triaxial tests) and load frame. The PC with the test software (not shown in the picture) is placed on the left hand side of the controller unit.*

is accomplished by means of a special testing software run on a PC connected to the controller. The load frame has a high stiffness and a fast responding actuator, cf the ISRM suggested method /1/.

The stiffness of the various components of the loading chain in the load frame has been optimized in order to obtain a high total stiffness. This includes the load frame, load cell, load platens and piston, as well as minimizing the amount of hydraulic oil in the cylinder. Furthermore, the sensors, the controller and the servo valve are rapidly responding components. The axial load is determined using a load cell, which has a maximum capacity of 1.5 MN. The uncertainty of the load measurement is less than 1%.

The axial and circumferential (radial) deformations of the rock specimens were measured. The rock deformation measurement systems are based on miniature LVDTs (electronic sensors), which have a measurement range of +/− 2.5 mm. The relative error for the LVDTs is less than 0.6% within a 1 mm range for the axial deformation measurements and less than 1.3% within a 3 mm range for the circumferential deformation measurement. The LVDTs have been calibrated by means of a micrometer.

Two independent systems were used for the axial deformation measurement in order to obtain two comparative results. The first system (S1), see Figure 3-2, comprises two aluminium rings attached to the specimen placed at ¼ and ¾ of the specimen height. Two LVDTs mounted on the rings are used to measure the distance change between the rings on opposite sides of the specimen. As to the attachment, a rubber band made of a thin rubber hose with 0.5 mm thickness is first mounted on the specimen right under where the rings are to be mounted. The rings have three adjustable spring-loaded screws, each with a rounded tip pointing on the specimen with 120 degrees division. The screw tips are thus pressing on the rubber band. The second system (S2), see Figure 3-3, consists of two aluminium plates that are clamped around the circular loading platens of steel on top and on bottom of the specimen. Two LVDTs, mounted on the plates, measure the distance change between these plates at opposite sides of the specimen at corresponding positions as for the first measurement system (S1).
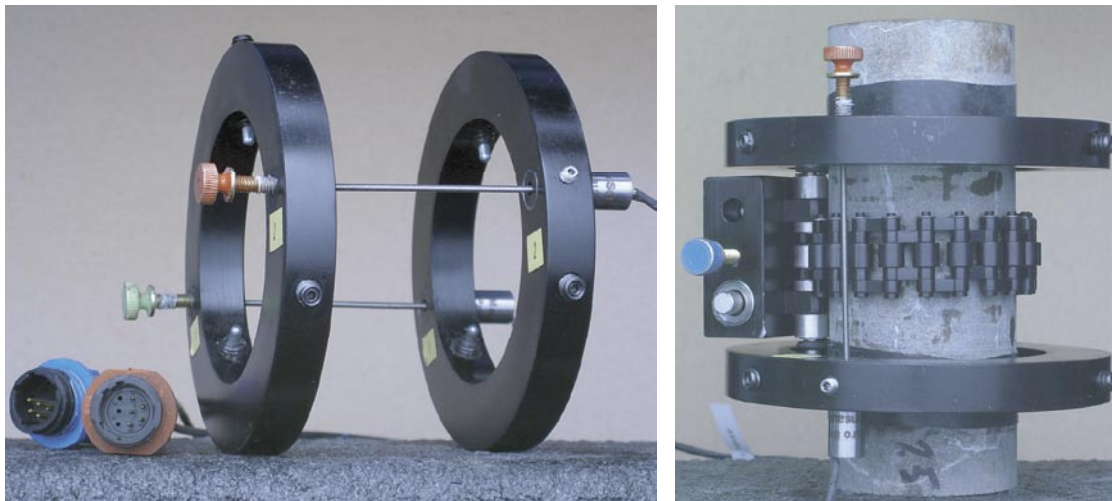
Figure 3-2. Left: Rings and LVDTs for local axial deformation measurement. Right: Specimen with two rubber bands. Devices for local axial and circumferential deformation measurements attached to the specimen.

The radial deformation was obtained by using a chain mounted around the specimen at mid-height, see Figures 3-2 and 3-3. The change of the chain-opening gap was measured by means of one LVDT and the circumferential and thereby also the radial deformation could be obtained. See Appendix A.

The specimens were photographed with a 4.0 Mega pixel digital camera at highest resolution and the photographs were stored in a jpeg-format.
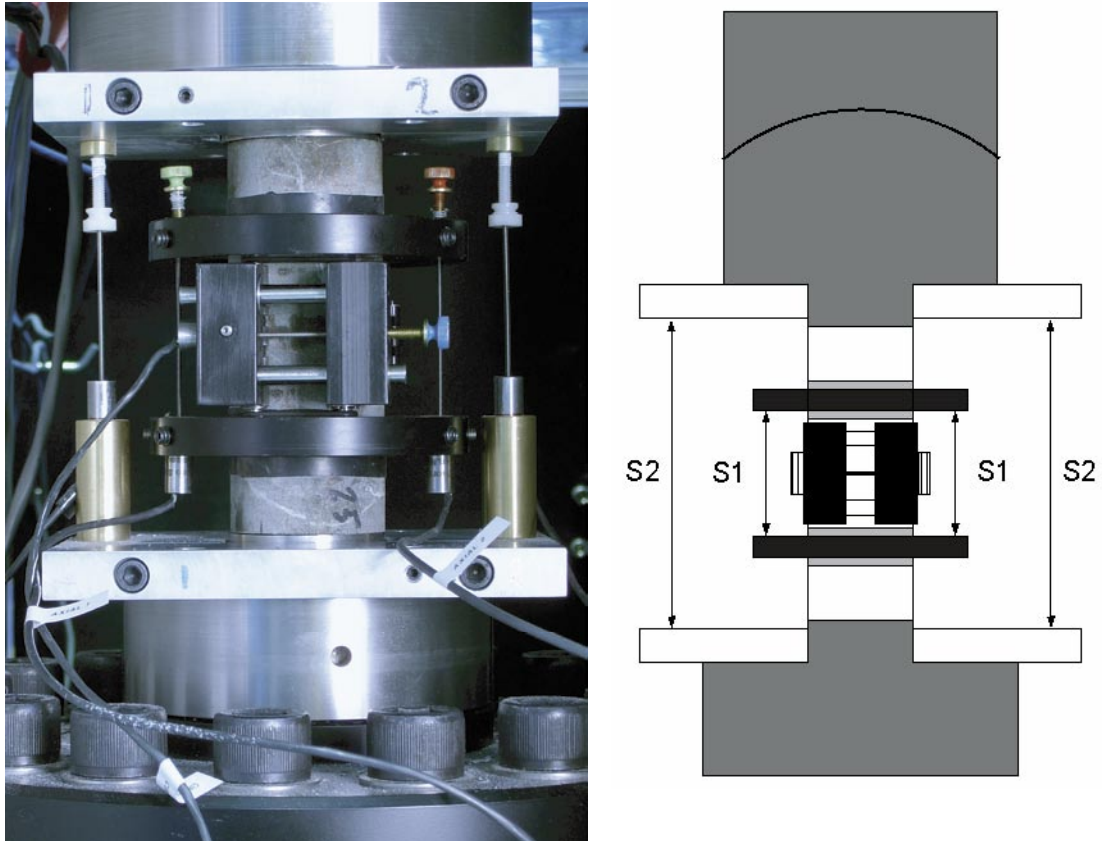
Figure 3-3. *Left: Specimen inserted between the loading platens. The two separate axial deformation measurement devices can be seen: system (S1) that measures the local axial deformation (rings) and system (S2) that measures the deformation between the aluminium plates (total deformation). Right: Principal sketch showing the two systems used for the axial deformation measurements.*

4   Execution

The water saturation and determination of the density of the wet specimens were made in accordance with the method description SKB MD 160.002, version 1.9 (SKB internal controlling document). This includes determination of density in accordance with ISRM /5/ and water saturation by SS EN 13755 /6/. The uniaxial compression tests were carried out in compliance with the method description SKB MD 190.001, version 1.9 (SKB internal controlling document). The test method is based on the ISRM suggested method /1/.

4.1   Description of the specimens

The rock type characterisation was made according to Stråhle /7/ using the SKB mapping system (Boremap). The identification marks, upper and lower sampling depth (Secup and Seclow) and the rock type are shown in Table 4-1.

Table 4-1. Specimen identification, sampling depth and rock type for all specimens.

Identification	Secup (m)	Seclow (m)	Rock type
KFM01A-113-1	225.92	226.07	Metagranodiorite-granite
KFM01A-113-2	226.09	226.24	(All specimens)
KFM01A-113-3	227.23	227.38	
KFM01A-113-4	228.00	228.15	
KFM01A-113-5	229.60	229.75	
KFM01A-113-8	496.01	496.15	
KFM01A-113-10	496.45	496.59	
KFM01A-113-12	496.74	496.88	
KFM01A-113-14	497.14	497.28	
KFM01A-113-16	497.42	497.57	
KFM01A-113-18	497.76	497.90	
KFM01A-113-20	690.32	690.46	
KFM01A-113-21	690.46	690.60	
KFM01A-113-22	690.60	690.74	
KFM01A-113-23	690.74	690.88	

4.2 Specimen preparation and density measurement

The temperature of the water was 19.0°C, which equals to a water density of 998.4 kg/m^3, when the determination of the wet density of the rock specimens was carried out. Further, the specimens had been stored 15 days in water when the density was determined.

A step-by step description of the procedure for the specimen preparation and the density measurement is as follows:

Step	Activity
1	The drill cores were marked where the specimens are to be taken.
2	The specimens were cut to the specified length according to markings and the cutting surfaces were grinded.
3	The tolerances were checked: parallel and perpendicular end surfaces, smooth and straight circumferential surface.
4	The diameter and height were measured three times each. The respective mean value determines the dimensions that are reported.
5	The specimens were then water saturated according to the method described in SKB MD 160.002, version 1.9, and were stored for minimum 7 days in water whereupon the wet density was determined.

4.3 Mechanical testing

The specimens had been stored 110–113 days in water when the uniaxial compression tests were carried out. The functionality of the testing system was checked by carrying out tests on other cores with a similar type rock before the tests described in this report started. A check-list was filled in successively during the work in order to confirm that the different specified steps had been carried out. Moreover, comments were made upon observations during the mechanical testing that are relevant for the interpretation of the results. The check-list form is a SP internal quality document.

A step-by step description of the test procedure is as follows:

Step	Activity
1	Digital photos were taken on each specimen before the mechanical testing.
2	Devices for measuring axial and circumferential deformations were attached to the specimen.
3	The specimen was put in place and centred between the frame loading platens.
4	The core on each LVDT was adjusted by means of a set screw to the right initial position. This was done so that the optimal range of the LVDTs can be used for the deformation measurement.
5	The frame piston was brought down into contact with the specimen with a force corresponding to 0.6 MPa axial stress.
6	A load cycle with loading up to 5 MPa and unloading to 0.6 MPa was conducted in order to settle possible contact gaps in the spherical seat in the piston and between the rock specimen and the loading platens.
7	The centring was checked again.
8	The deformation measurement channels were zeroed in the test software.
9	The loading was started and the initial loading rate was set to a radial strain rate of –0.025%/min. The loading rate was increased after reaching the post-failure region. This was done in order to prevent the total time for the test to become too long.
10	The test was stopped either manually when the test had proceeded long enough to reveal the post-failure behaviour, or after severe cracking had occurred and it was judged that very little residual axial loading capacity was left in the specimen.
11	Digital photos were taken on each specimen after the mechanical testing.

4.4   Data handling

The test results were exported as text files from the test software and stored in a file server on the SP computer network after each completed test. The main data processing, in which the elastic moduli were computed and the peak stress was determined, has been carried out in the program MATLAB /8/. Moreover, MATLAB was used to produce the diagrams shown in Section 5.1 and in Appendix B. The summary of results in Section 5.2 with tables containing mean value and standard deviation of the different parameters and diagrams were produced using MS Excel. MS Excel was also used for reporting data to the SICADA database.

4.5   Analyses and interpretation

As to the definition of the different result parameters we begin with the axial stress σ_a, which is defined as

$$\sigma_a = \frac{F}{A}$$

where F is the axial force acting on the specimen and A is the specimen cross section area. The peak value of the axial stress during a test is representing the uniaxial compressive strength σ_c in the results presentation.

The average value of the two axial displacement measurements on opposite sides of the specimen is used for the axial strain calculation, cf Figure 3-3. In the first measurement system (S1), the recorded deformation represents a local axial deformation δ_{local} between the points at ¼ and ¾ height. A local axial strain is defined as

$$\varepsilon_{a,local} = \delta_{local}/L_{local}$$

where L_{local} is the distance between the rings before loading.

In the second measurement system (S2), the recorded displacement corresponds to a total deformation that, in addition to the total rock deformation, also contains the local deformations that occur in the contact between the rock and the loading platens and further also the deformation of the steel loading platens at each side of the specimen ends. The average value of the two total deformation measurements on opposite sides of the specimen is defined as the total deformation δ_{total}. An axial strain based on the total of the deformation is defined as

$$\varepsilon_{a,total} = \delta_{total}/L_{total}$$

where L_{total} is the height of the rock specimen.

The radial deformation is measured by means of a chain mounted around the specimen at mid-height, cf Figures 3-2 and 3-3. The change of the chain opening gap is measured by means of an LVDT. This measurement is used to compute the radial strain ε_r, see Appendix A. Moreover, the volumetric strain ε_{vol} is defined as

$$\varepsilon_{vol} = \varepsilon_a + 2\varepsilon_r$$

17

The stresses and the strains are defined as positive in compressive loading and deformation. The elasticity parameters are defined by the tangent Young's modulus E and tangent Poisson ratio v as

$$E = \frac{\sigma_a(0.55\sigma_c) - \sigma_a(0.45\sigma_c)}{\varepsilon_a(0.55\sigma_c) - \varepsilon_a(0.45\sigma_c)}$$

$$v = -\frac{\varepsilon_r(0.55\sigma_c) - \varepsilon_r(0.45\sigma_c)}{\varepsilon_a(0.55\sigma_c) - \varepsilon_a(0.45\sigma_c)}$$

The tangents were evaluated with values corresponding to an axial load between 45% and 55% of the axial peak stress σ_c.

Two important observations can be made from the results:

(i)   The results based on the total axial deformation measurement (S2) display a lower axial stiffness, i.e. a lower value on Young's modulus, than in the case when the results are based on the local axial deformation measurement (S1). This is due to the additional deformations from the contact interface between the rock specimen and the steel loading platens and also due to the deformation of the loading platens themselves.

(ii) It can be seen that the response differs qualitatively between the results obtained with the local axial deformation measurement system (S1) and the system that measure total axial deformation (S2). In some cases the post-peak response obtained with the local deformation measurement system seems not to be physically correct. This can be due to a number of reasons, e.g. that a crack caused a local deformation, see Figure 4-1. Another explanation could be that the rings attached to the specimens have slightly slipped or moved, for example if a crack was formed nearby one of the attachment points.

It is reasonable to assume that results based on the local axial deformation measurement (S1) are fairly accurate up to the formation of the first macro cracks or up to the peak load, but not after. However, the results obtained with the total axial deformation measurement (S2) seem to be qualitatively correct after failure. We will therefore report the results based on the total axial deformation measurement, but carry out a correction of those results as described below in order to get overall good results.
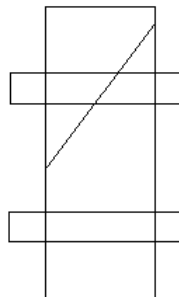
Figure 4-1. *Example of cracking that may cause results that are difficult to interpret from a local deformation measurement.*

The total axial deformation δ_{total} measured by (S2) is a summation of several deformations

$$\delta_{total} = \delta_{rock} + \delta_{system} \tag{1}$$

where

$$\delta_{system} = \delta_{interface} + \delta_{loading\ platens}$$

and δ_{rock} is the axial deformation of the whole rock specimen. Assume that the system deformation is proportional to the applied axial force F_a in the loading chain, i.e.

$$\delta_{system} = F_a/K_{system} \tag{2}$$

where K_{system} is the axial stiffness in the system (containing the interface between the rock and loading platens and the deformation of the loading platens). Combining (1) and (2) leads to

$$\delta_{rock} = \delta_{total} - F_a/K_{system} \tag{3}$$

where an expression of the axial deformation of the entire specimen is obtained. This can be viewed as a correction of the measurements made by system (S2). By using δ_{rock} to represent the axial deformation of the specimen that is based on a correction of the results of the total axial deformation will yield good results both in the loading range up to failure and also at loading after failure. However, it is noticed that K_{system} is not known and has to be determined.

It was previously suggested that the local axial deformation measurement represents the real rock deformation well up to the load where the macro cracks develop. Further, it is fair to assume that the axial deformation is homogenous at this part of the loading. Hence, we get

$$\delta_{rock} = \delta_{local} \cdot L_{total}/L_{local}$$

This yields representative values of the total rock deformation for the first part of the loading up to the point where macro cracking is taking place. By rewriting (2) we get

$$K_{system} = \frac{F_a}{\delta_{system}} \tag{4}$$

It is now possible to determine δ_{system} up to the threshold of macro cracking. We will, however, compute the system stiffness based on the results between 45% and 55% of the axial peak stress σ_c. This means that the Young's modulus and the Poisson ratio will take the same values both when the data from the local axial deformation measurement (S1) and when the data from corrected total axial deformation are used. This means

$$K_{system} = \frac{F_a(0.55\,\sigma_c) - F_a(0.45\,\sigma_c)}{\delta_{system}(0.55\sigma_c) - \delta_{system}(0.45\sigma_c)} \tag{5}$$

where $\delta_{system} = \delta_{total} - \delta_{rock}$ according to (1). The results based on the correction according to (3) and (5) are presented in Section 5.1 whereas the original measured unprocessed data are reported in Appendix B.

A closure of present micro cracks will take place initially during axial loading. Development of new micro cracks will start when the load is further increased and axial stress reaches the crack initiation stress σ_i. The crack growth at this stage is as stable as increased loading is required for further cracking. A transition from a development of micro cracks to macro cracks will take place when the axial load is further increased. At a certain stress level the crack growth becomes unstable. The stress level when this happens is denoted the crack damage stress σ_d, cf /2/. In order to determine the stress levels we look at the volumetric strain.

By subtracting the elastic volumetric strain ε_{vol}^{e} from the total volumetric strain, a volumetric strain corresponding to the crack volume ε_{vol}^{cr} is obtained. This has been denoted calculated crack volumetric strain in the literature, cf /2, 3/. We have thus

$$\varepsilon_{vol}^{cr} = \varepsilon_{vol} - \varepsilon_{vol}^{e}$$

Assuming linear elasticity leads to

$$\varepsilon_{vol}^{cr} = \varepsilon_{vol} - \frac{1-2\nu}{E}\sigma_a$$

where $\sigma_r = 0$ was used. Experimental investigations have shown that the crack initiation stress σ_i coincides with the onset of increase of the calculated crack volume, cf /2, 3/. The same investigations also indicate that the crack damage stress σ_d can be defined as the axial stress at which the total volume starts to increase, i.e. when a dilatant behaviour is observed.

5 Results

The results of the individual specimens are presented in Section 5.1 and a summary of the results is given in Section 5.2. The reported parameters are based both on unprocessed raw data obtained from the testing and processed data and were reported to the SICADA database, field note no Forsmark 96. These data together with the digital photographs of the individual specimens were stored on a CD and handed over to SKB. The handling of the results follows SDP-508 (SKB internal controlling document) in general.

5.1 Results of individual specimens

The cracking is shown in pictures of the specimens and comments on observations that appeared during the testing are reported. The elasticity parameters have been evaluated by using the results from the local axial deformation measurements. The data from the adjusted total axial deformation measurements, cf Section 4.4, are also shown in this section. Red rings are superposed on the graphs indicating every five minutes of the progress of testing.

Diagrams showing the data from both the local and the total axial deformation measurements, system (S1) and (S2) in Figure 3-3, and the computed individual values of K_{system} used at the data corrections are shown in Appendix B. The diagrams with actual radial strain rates versus the test time are also presented in Appendix B. The results for the individual specimens are as follows:

Specimen ID: KFM01A-113-1

Before mechanical test   After mechanical test
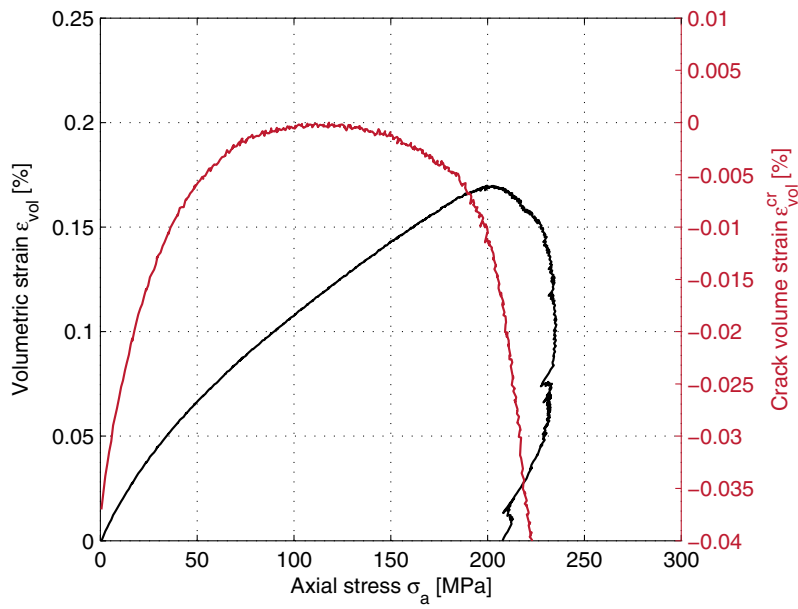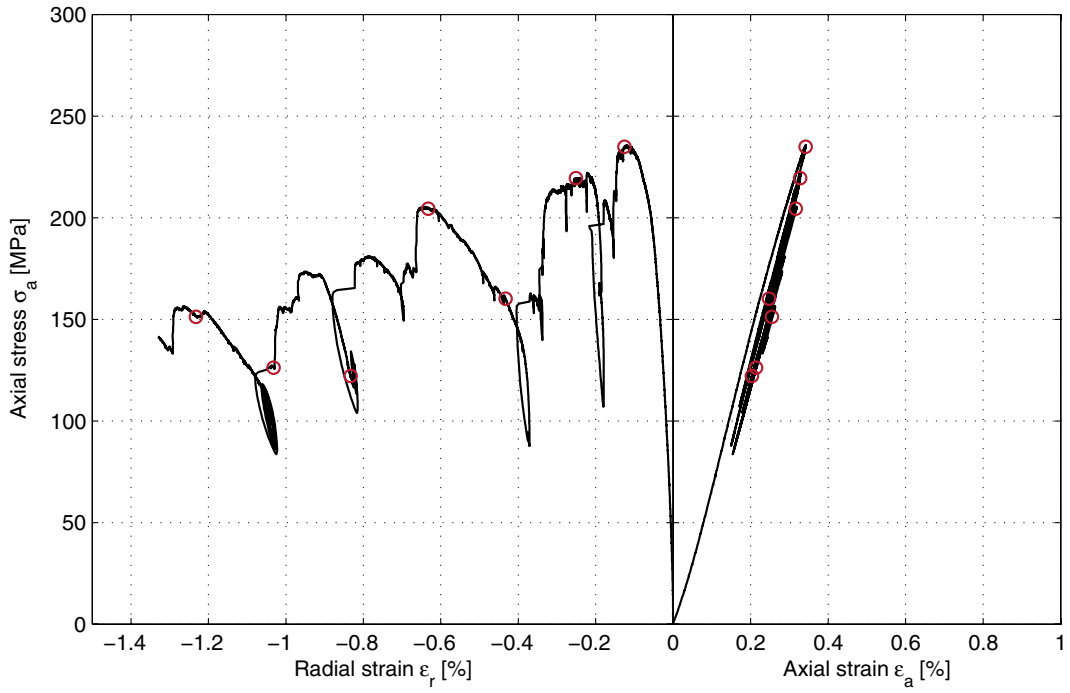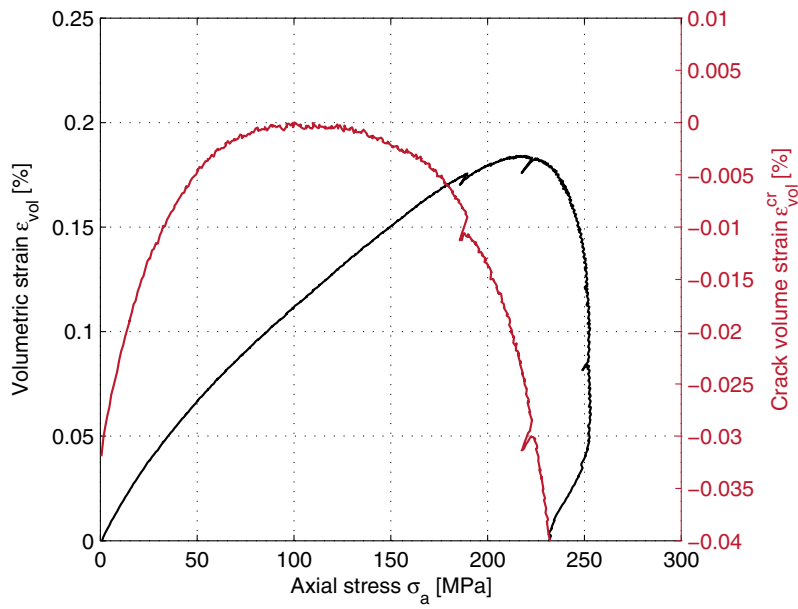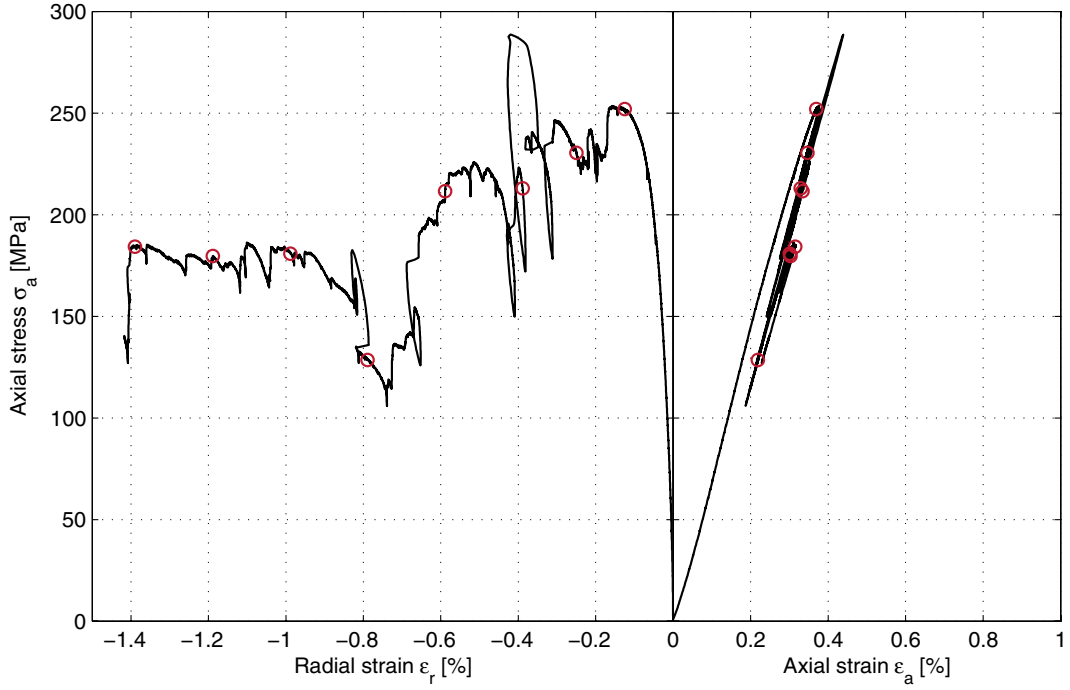

Diameter (mm)	Height (mm)	Density (kg/m³)
50.8	121.8	2,660

Comments   Spalling on one side of the specimen along the foliation. The test was restarted after the first major cracking.

Specimen ID: KFM01A–113–01

Youngs Modulus (E):	81.9	[GPa]
Poisson Ratio (ν):	0.24	[–]
Axial peak stress (σ_c):	270.1	[MPa]
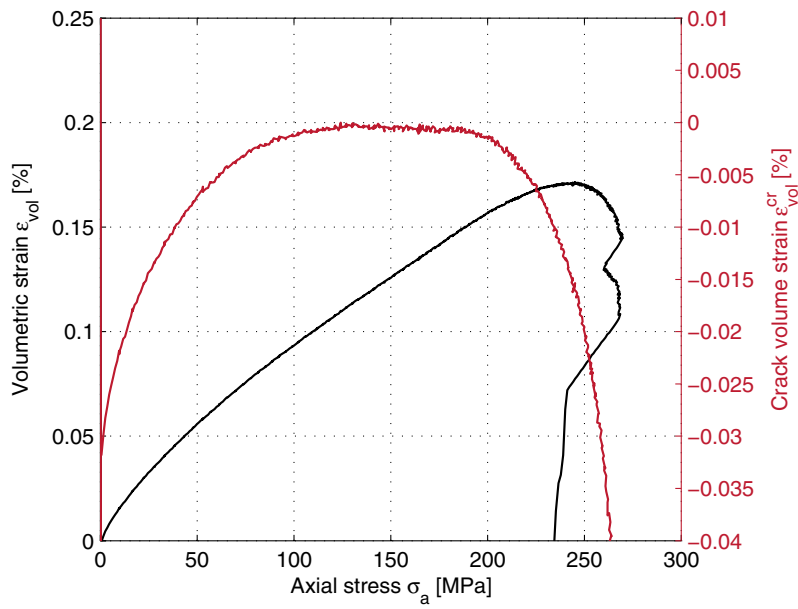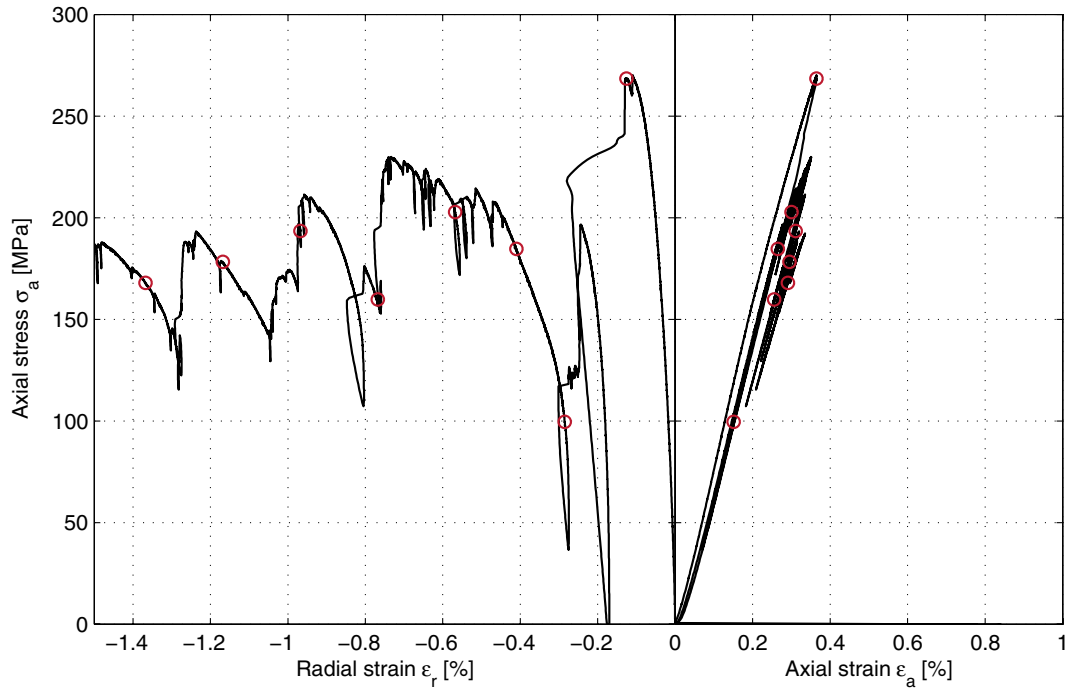
Specimen ID: KFM01A-113-2

Before mechanical test   After mechanical test

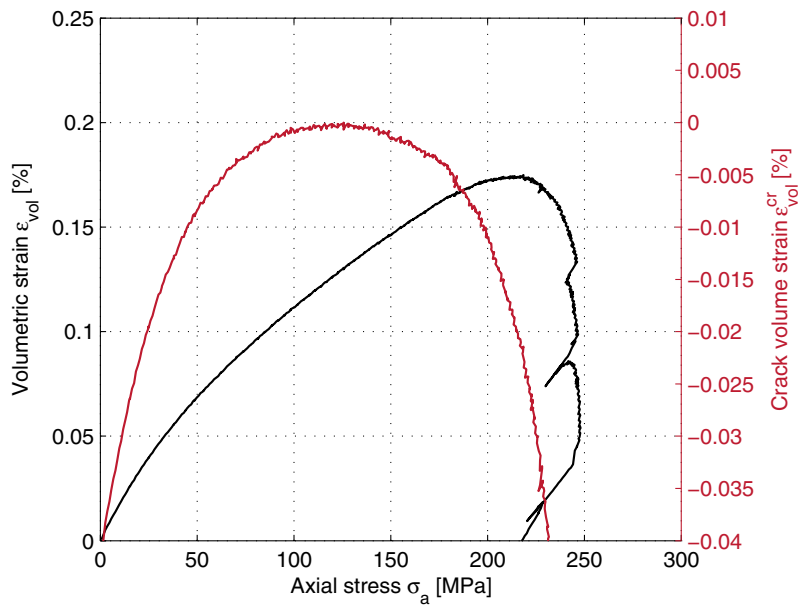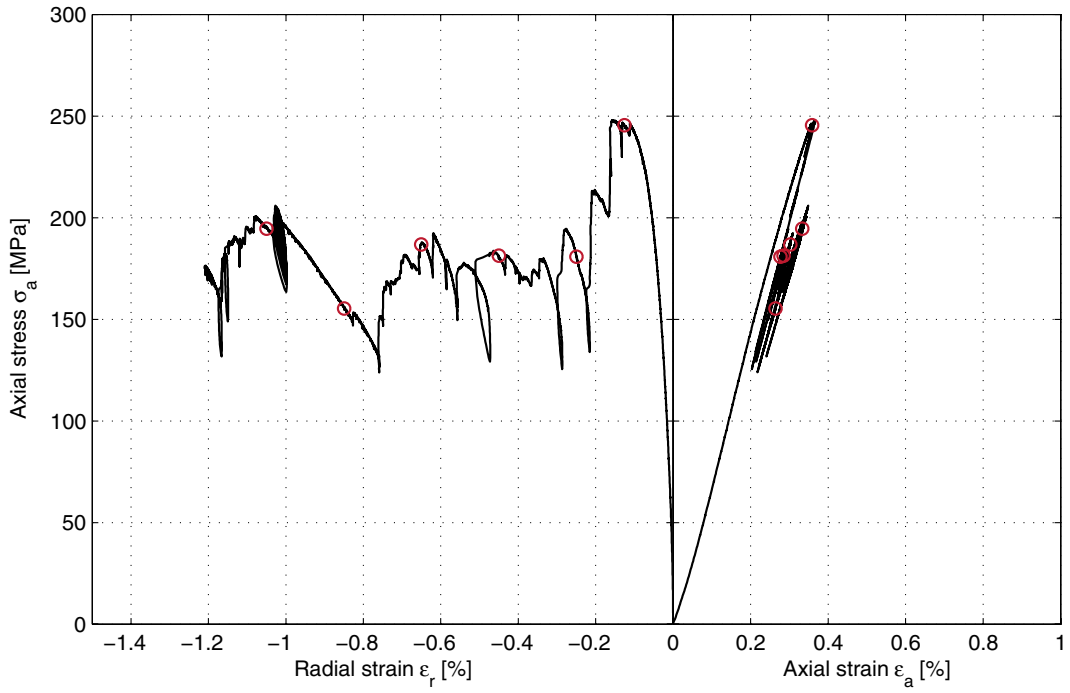| Diameter (mm)	Height (mm)	Density (kg/m³)
50.8	127.5	2,660

Comments	Spalling on both sides of the specimen along the foliation.

Specimen ID: KFM01A–113–02

Youngs Modulus (E):	78.1	[GPa]
Poisson Ratio (ν):	0.207	[−]
Axial peak stress (σ_c):	269.7	[MPa]
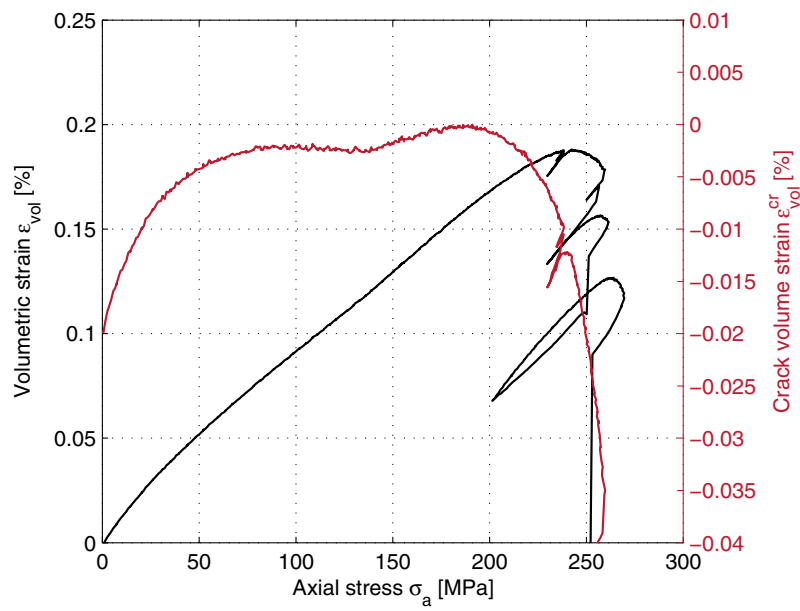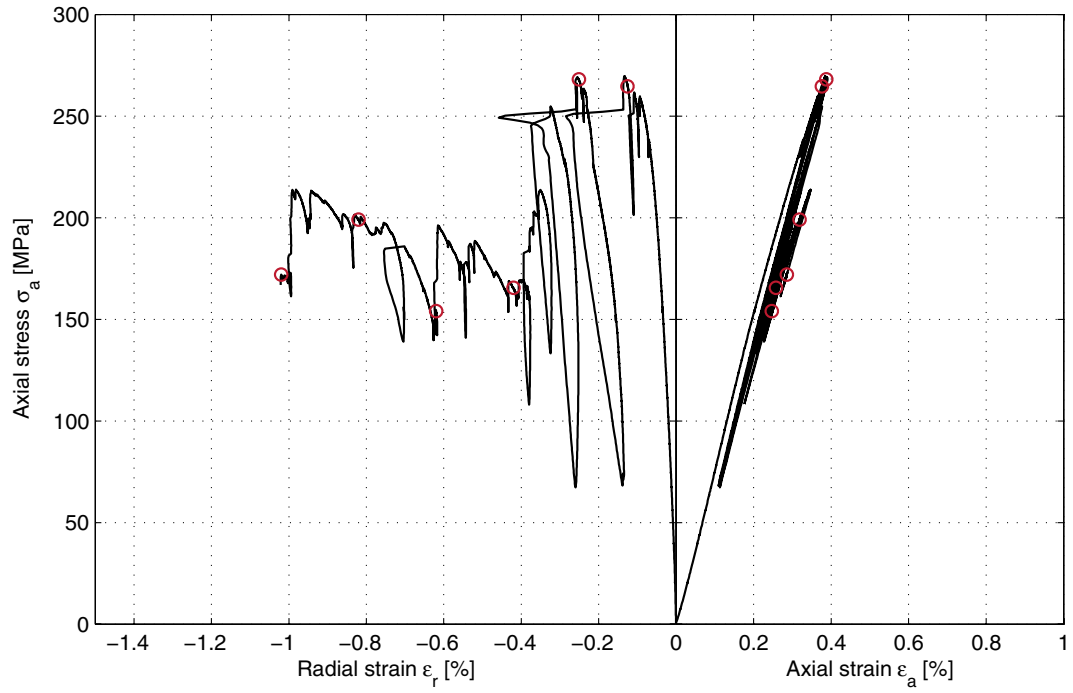
Specimen ID: KFM01A-113-3

Before mechanical test   After mechanical test
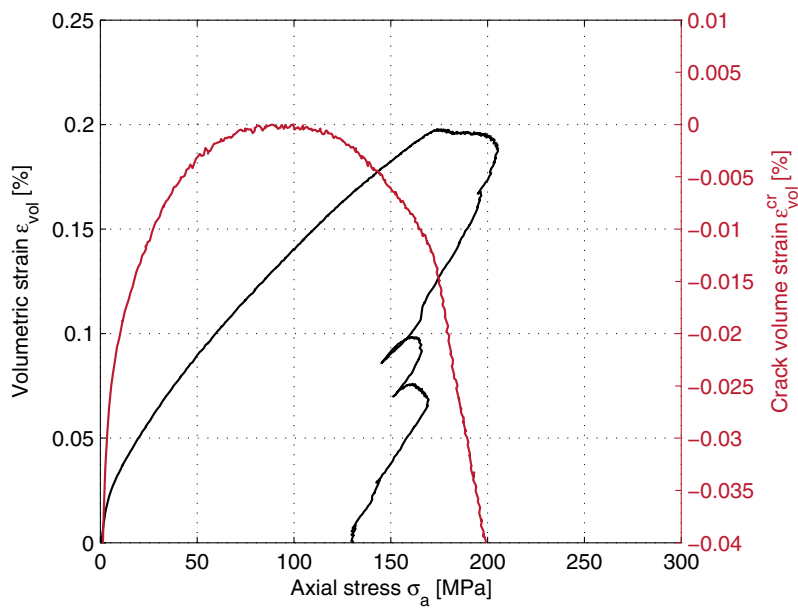

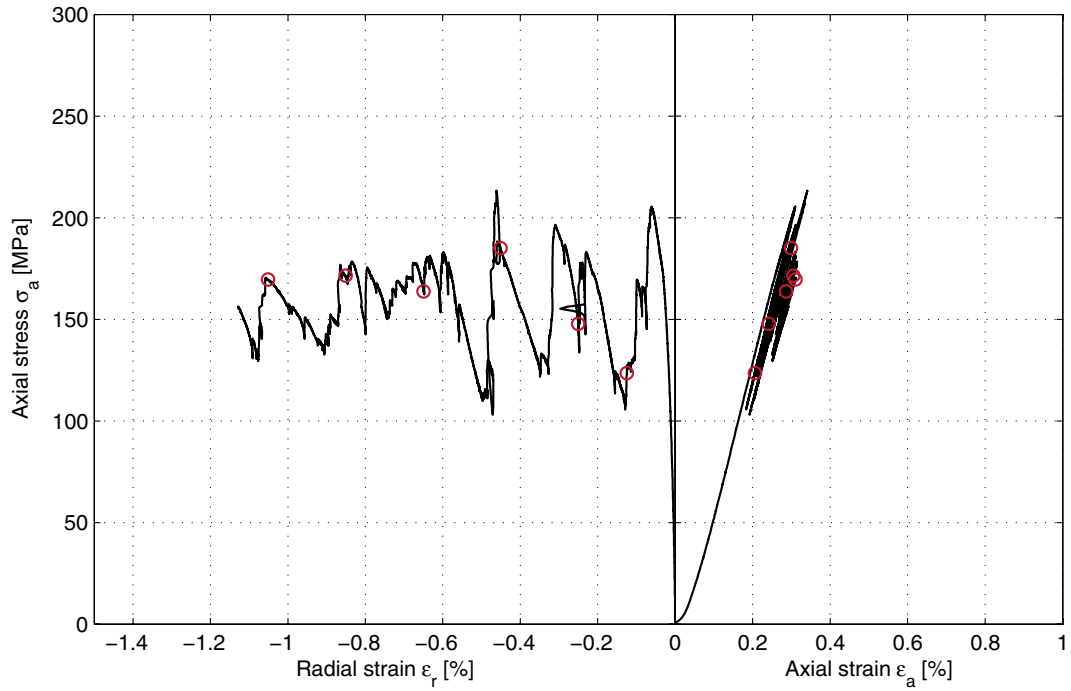| Diameter (mm)	Height (mm)	Density (kg/m³)
50.8	127.5	2,650

Comments   Spalling on both sides of the specimen along the foliation.

Specimen ID: KFM01A–113–03

Youngs Modulus (E):	79.1	[GPa]
Poisson Ratio (ν):	0.255	[–]
Axial peak stress (σ$_c$):	220.4	[MPa]
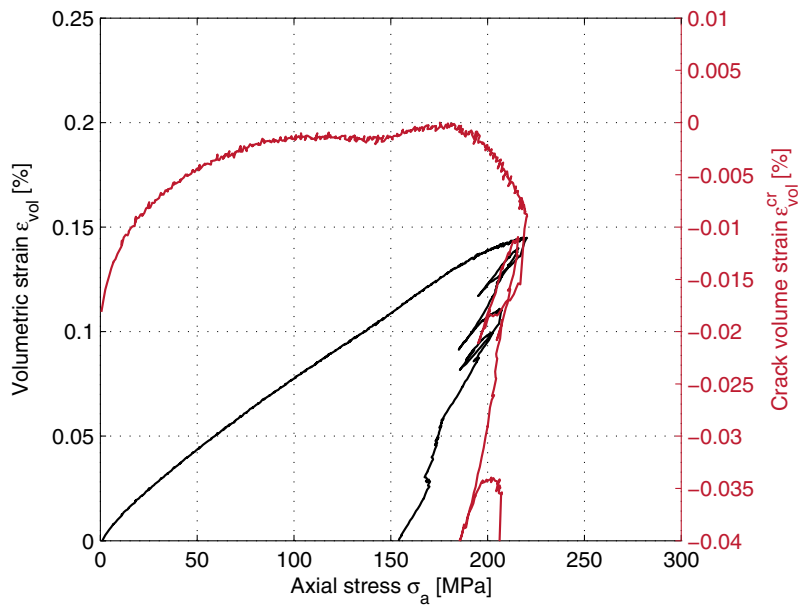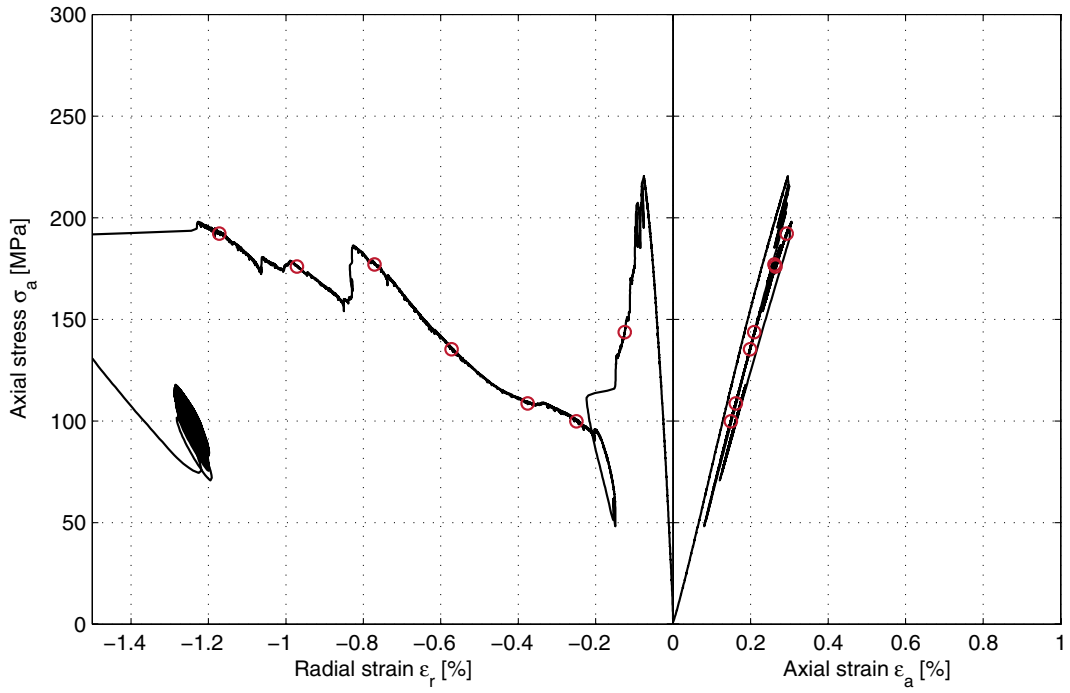
Specimen ID: KFM01A-113-4

Before mechanical test   After mechanical test

| Diameter (mm)	Height (mm)	Density (kg/m³)
50.6	127.0	2,660

Comments   Spalling on both sides of the specimen along the foliation.

Specimen ID: KFM01A–113–04

Youngs Modulus (E):	74	[GPa]
Poisson Ratio (ν):	0.217	[–]
Axial peak stress (σ$_c$):	224.1	[MPa]
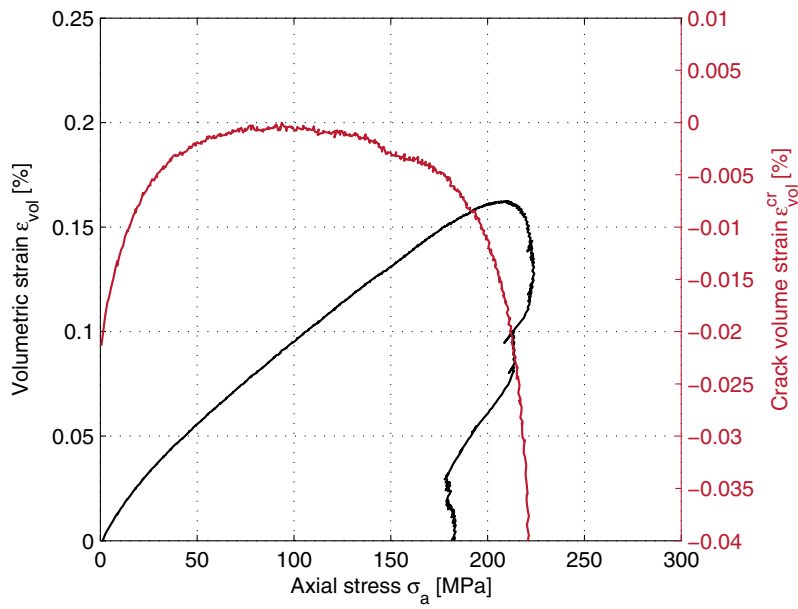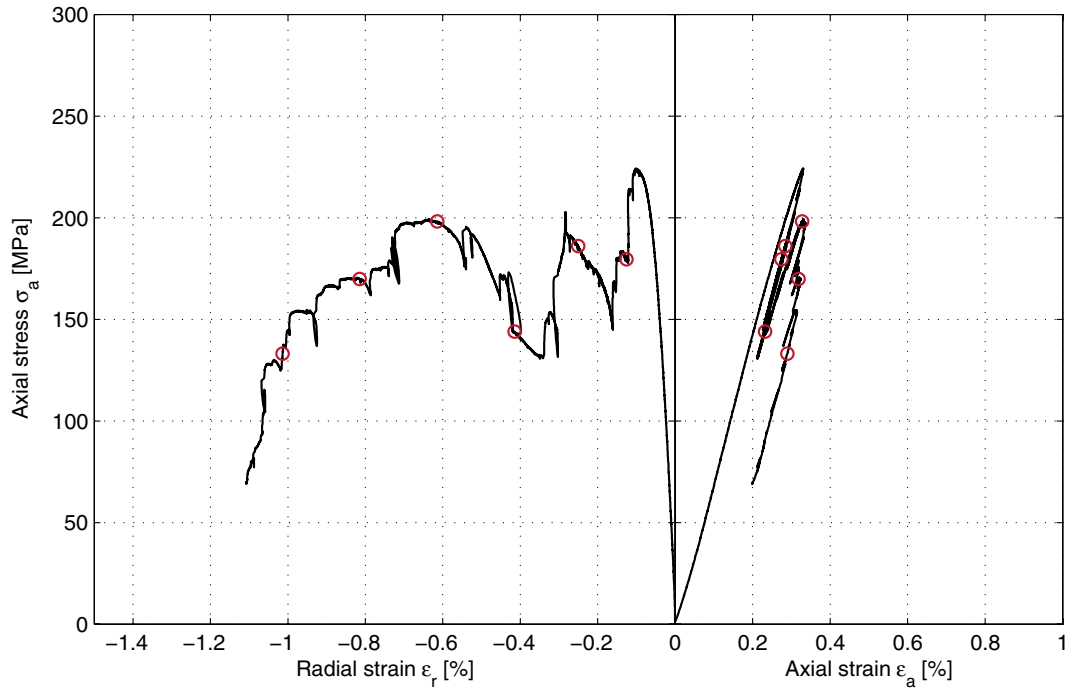
Specimen ID: KFM01A-113-5

Before mechanical test   After mechanical test
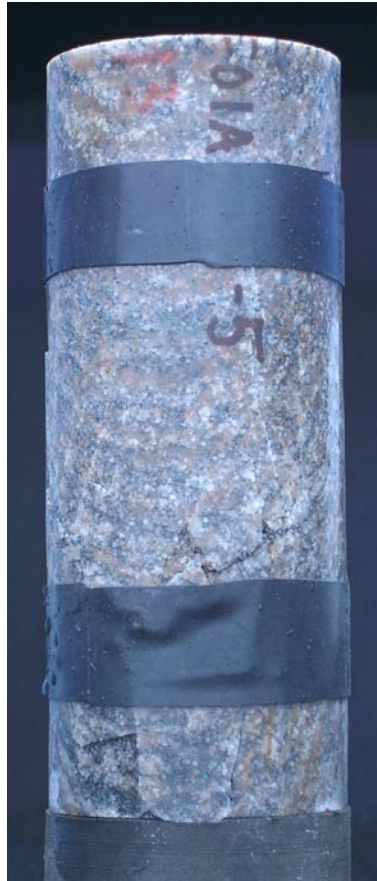
Diameter (mm)	Height (mm)	Density (kg/m³)
50.6	127.5	2,650

Comments   Spalling on one side of the specimen along the foliation.

Specimen ID: KFM01A–113–05

Youngs Modulus (E):	79.8	[GPa]
Poisson Ratio (ν):	0.278	[–]
Axial peak stress (σ_c):	227	[MPa]
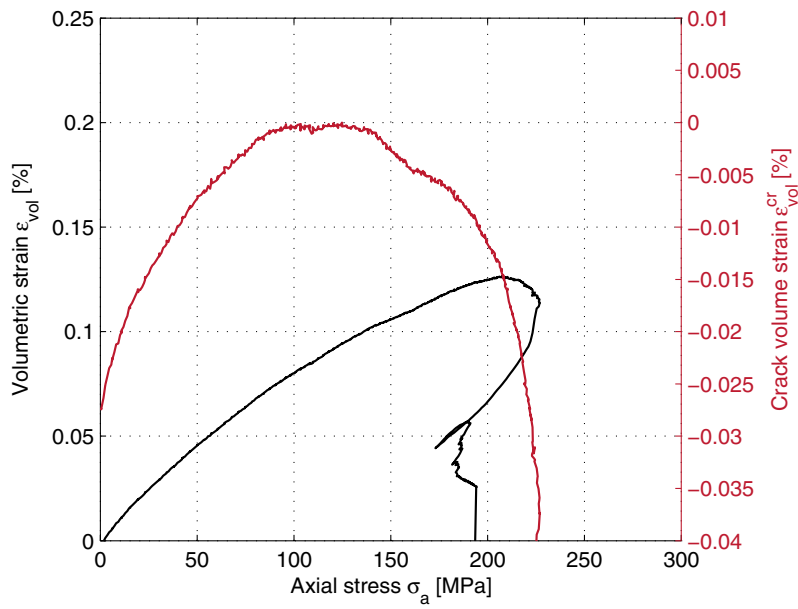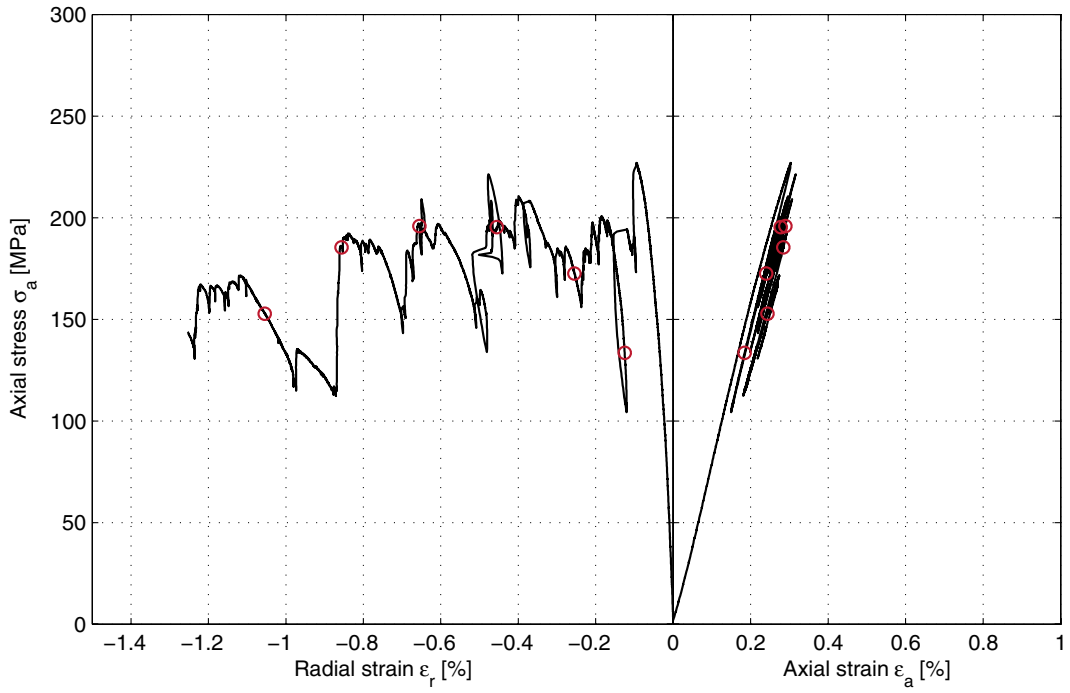
Specimen ID: KFM01A-113-8

Before mechanical test   After mechanical test
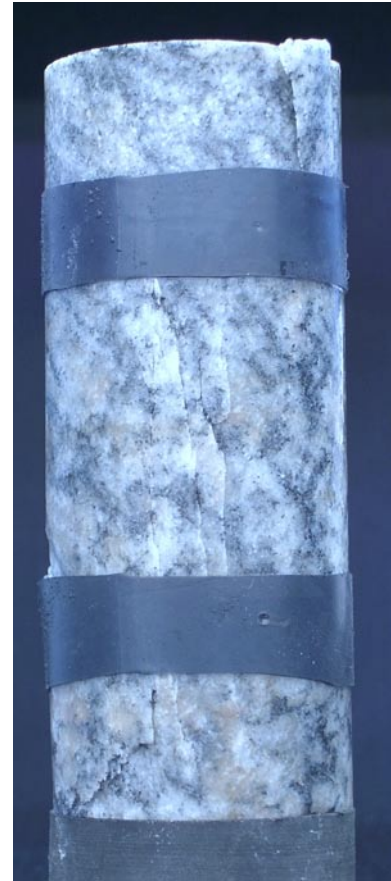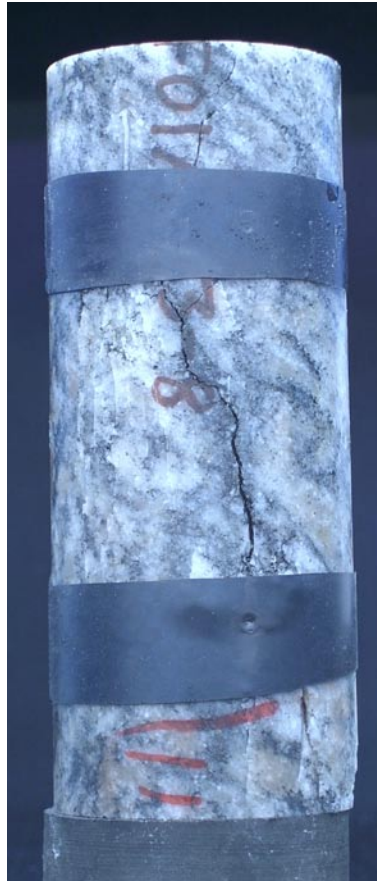
Diameter (mm)	Height (mm)	Density (kg/m³)
50.7	126.7	2,660

Comments	Deep vertical curved (cone-shaped) crack on one side of the specimen.

Specimen ID: KFM01A−113−08

Youngs Modulus (E):	78.9	[GPa]
Poisson Ratio (ν):	0.237	[−]
Axial peak stress (σ$_c$):	187.4	[MPa]
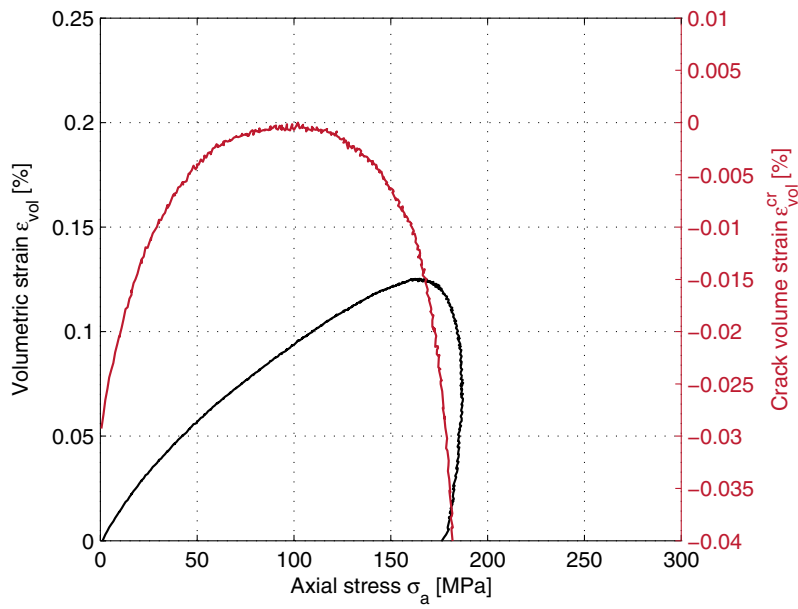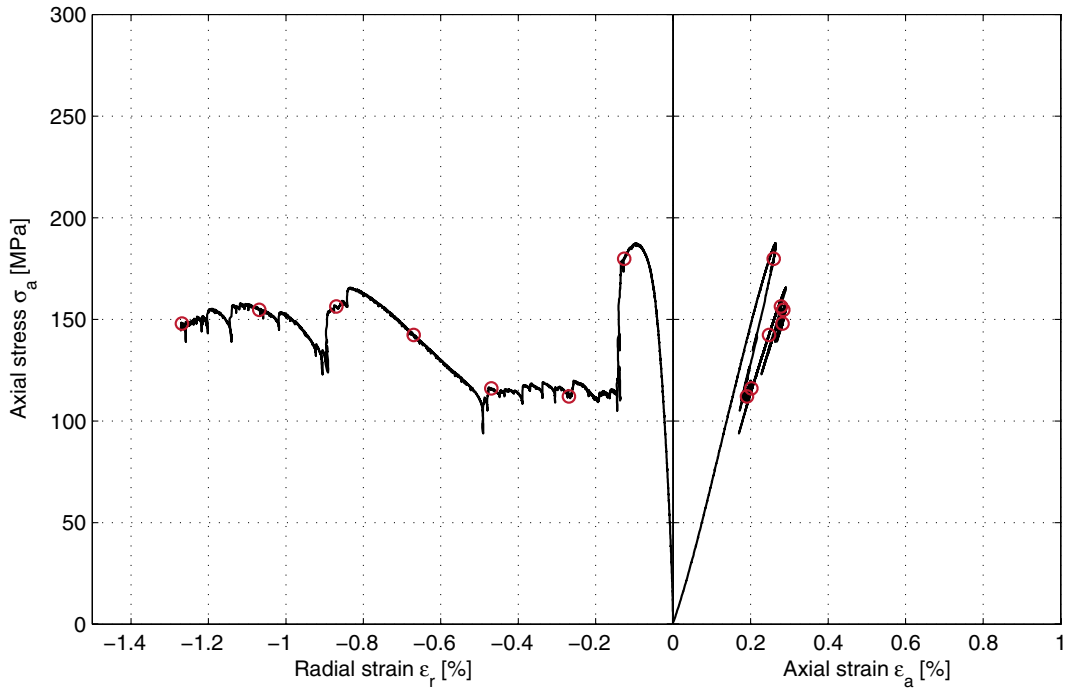
Specimen ID: KFM01A-113-10

Before mechanical test   After mechanical test

Diameter (mm)	Height (mm)	Density (kg/m³)
50.7	126.9	2,650

Comments	Spalling on one side and vertical cracks on the other side of the specimen along the foliation.

Specimen ID: KFM01A–113–10

Youngs Modulus (E):	76.1	[GPa]
Poisson Ratio (ν):	0.199	[–]
Axial peak stress (σ_c):	229.3	[MPa]
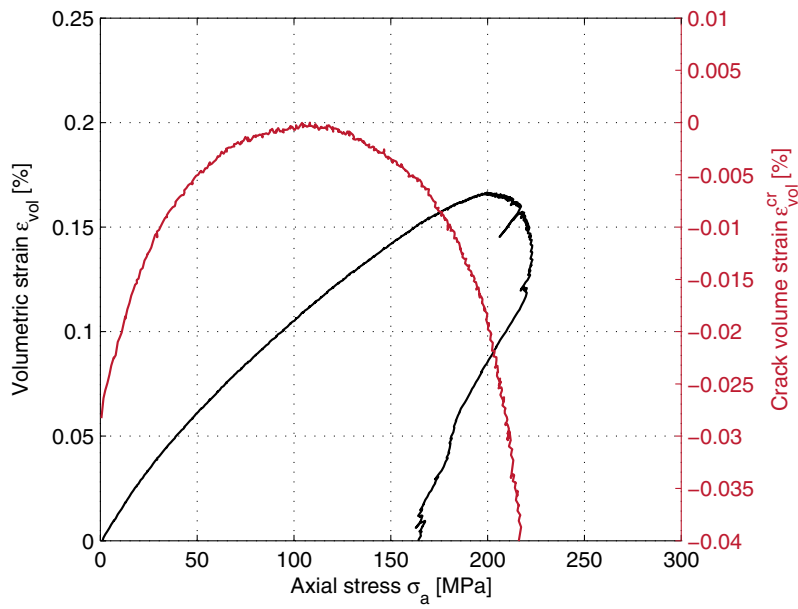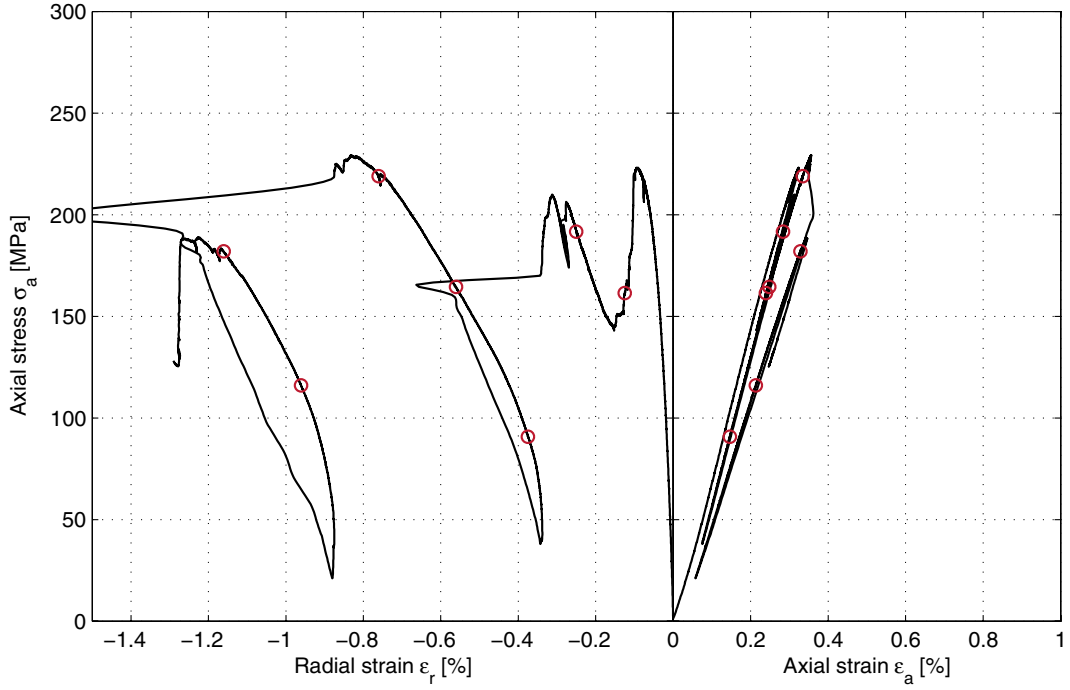
Specimen ID: KFM01A-113-12

Before mechanical test   After mechanical test
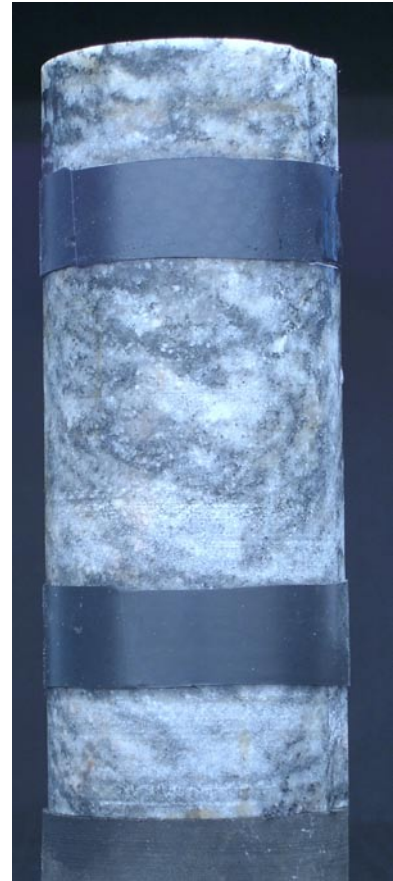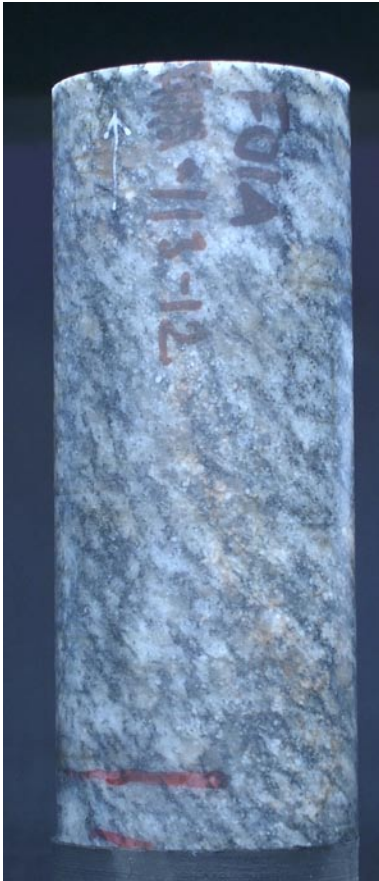
Diameter (mm)	Height (mm)	Density (kg/m³)
50.8	126.7	2,660

Comments   Vertical cracks on one side of the specimen along the foliation.

Specimen ID: KFM01A−113−12

Youngs Modulus (E):	76.5	[GPa]
Poisson Ratio (ν):	0.222	[−]
Axial peak stress (σ_c):	261.6	[MPa]
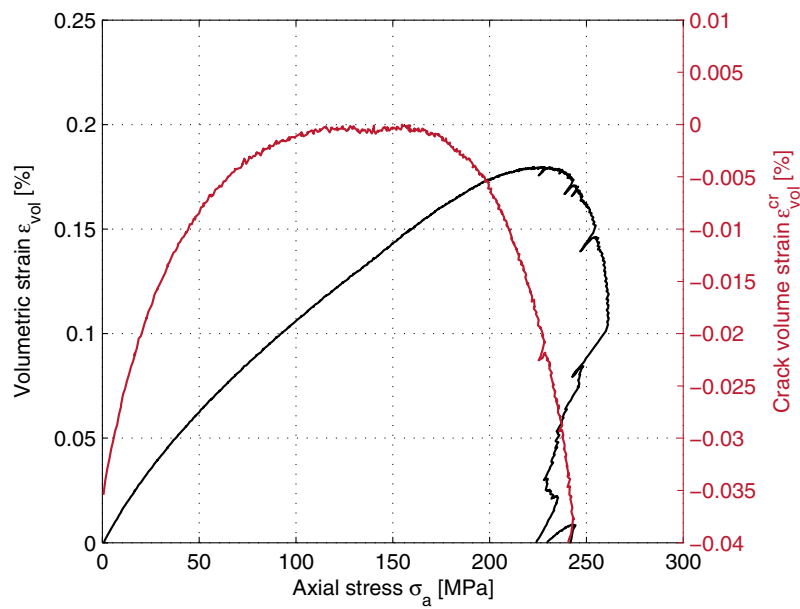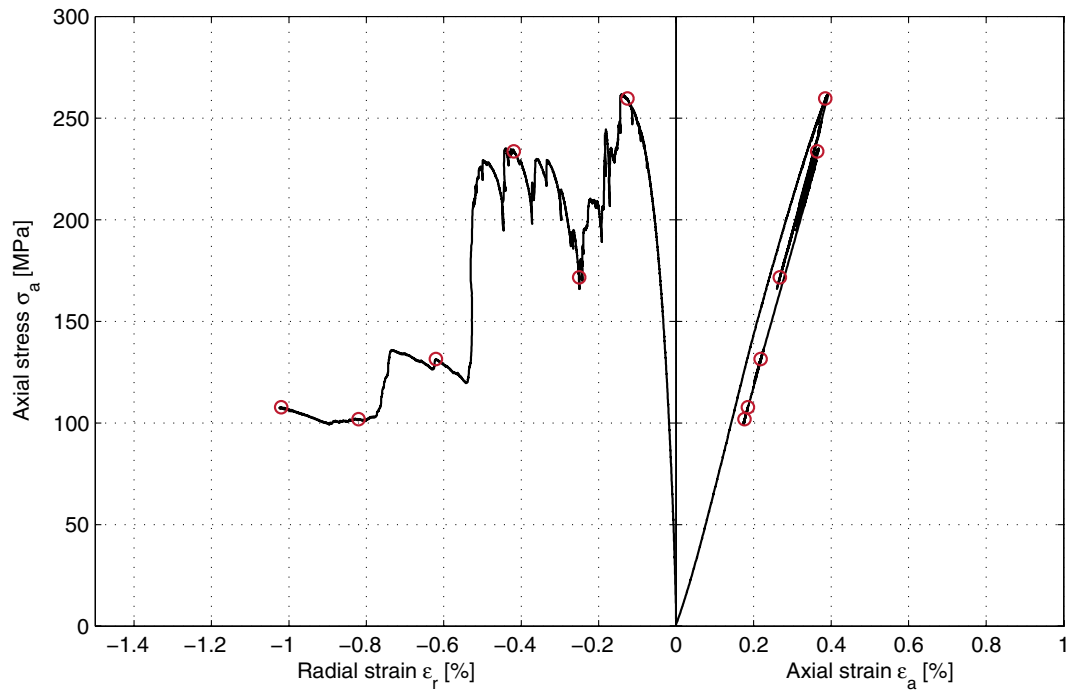
Specimen ID: KFM01A-113-14

Before mechanical test   After mechanical test

Diameter (mm)	Height (mm)	Density (kg/m³)
50.5	126.7	2,660

Comments	Spalling on one side of the specimen along the foliation. The test was stopped after the cracking as a large radial deformation was recorded.

Specimen ID: KFM01A−113−14

Youngs Modulus (E):	74.2	[GPa]
Poisson Ratio (ν):	0.181	[−]
Axial peak stress (σ$_c$):	238.9	[MPa]
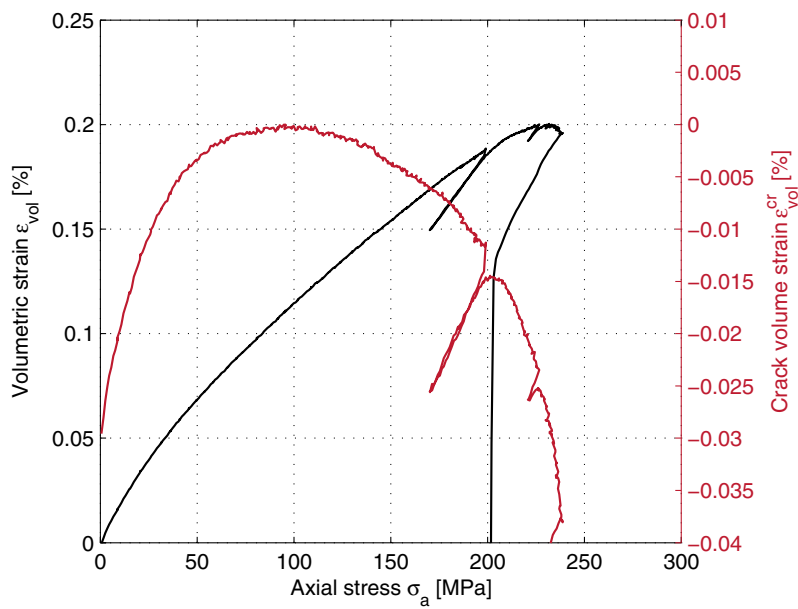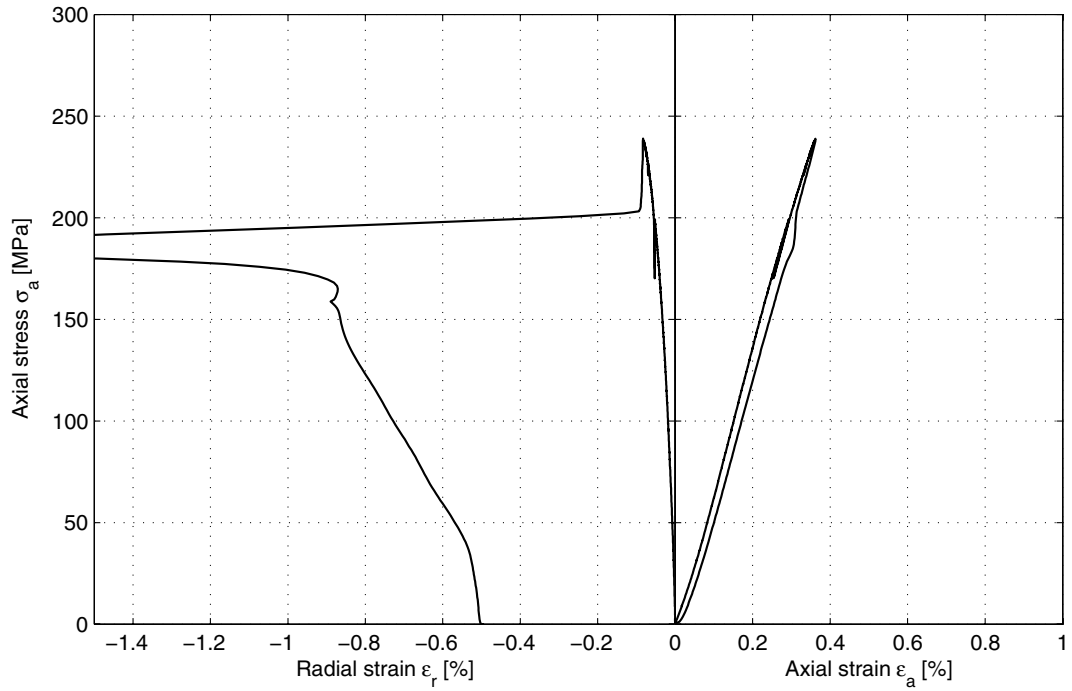
Specimen ID: KFM01A-113-16

Before mechanical test   After mechanical test

Diameter (mm)	Height (mm)	Density (kg/m³)
50.7	126.6	2,660

Comments   Spalling on both sides of the specimen along the foliation.

Specimen ID: KFM01A–113–16

Youngs Modulus (E):	75.3	[GPa]
Poisson Ratio (ν):	0.23	[–]
Axial peak stress (σ_c):	235.6	[MPa]

Specimen ID: KFM01A-113-18

Before mechanical test

After mechanical test
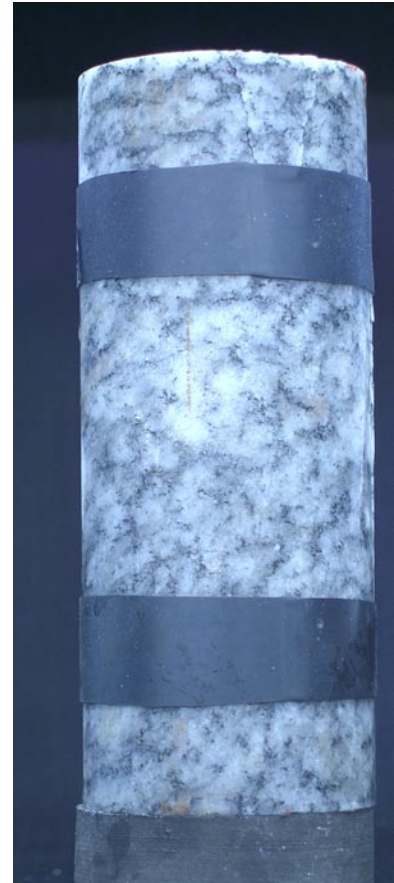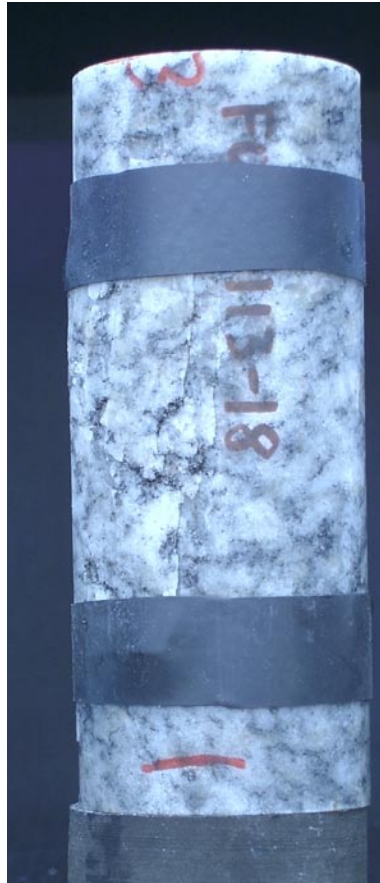
Diameter (mm)	Height (mm)	Density (kg/m³)
50.7	127.4	2,660

Comments	Spalling in the longitudinal direction not along the foliation.

Specimen ID: KFM01A-113-18

Youngs Modulus (E):	78	[GPa]
Poisson Ratio (ν):	0.184	[–]
Axial peak stress (σ_c):	288.6	[MPa]

Specimen ID: KFM01A-113-20

Before mechanical test   After mechanical test

Diameter (mm)	Height (mm)	Density (kg/m³)
51.1	121.9	2,660

Comments   Spalling on one side of the specimen along the foliation.

Specimen ID: KFM01A–113–20

Youngs Modulus (E):	77.8	[GPa]
Poisson Ratio (ν):	0.265	[–]
Axial peak stress (σ$_c$):	224.6	[MPa]
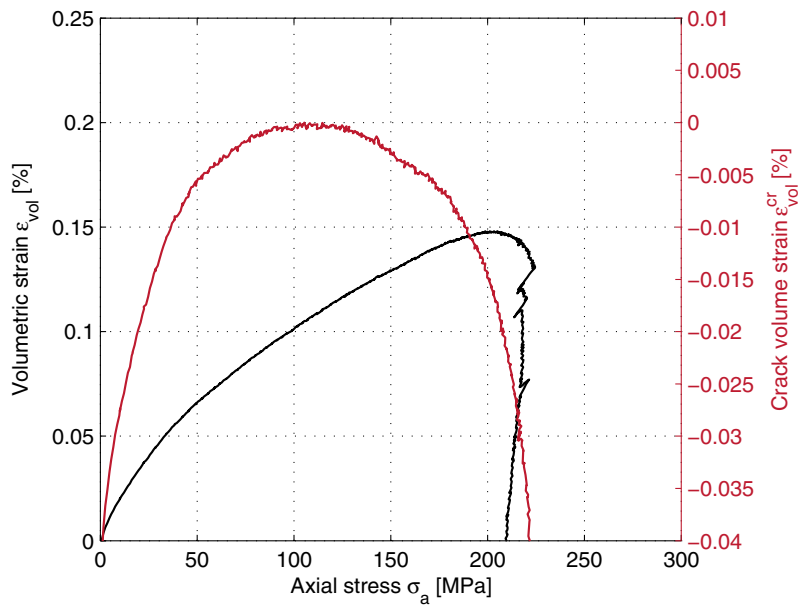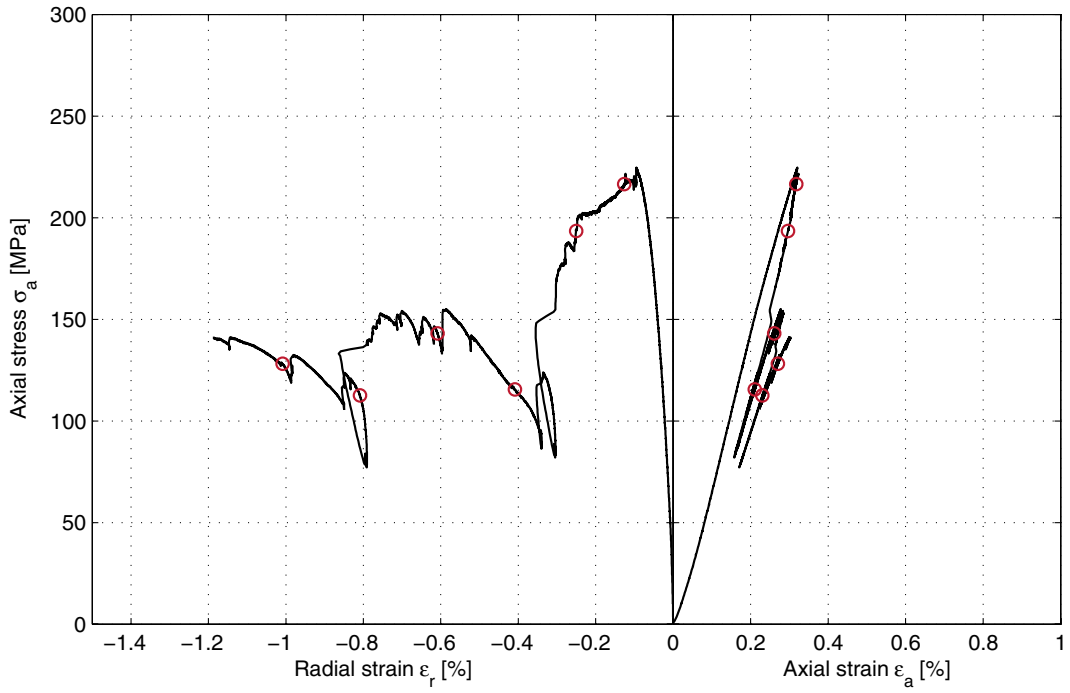
Specimen ID: KFM01A-113-21

Before mechanical test   After mechanical test

Diameter (mm)	Height (mm)	Density (kg/m³)
51.1	127.0	2,650

Comments   Spalling on one side of the specimen along the foliation.

Specimen ID: KFM01A−113−21

Youngs Modulus (E):	76.5	[GPa]
Poisson Ratio (ν):	0.229	[−]
Axial peak stress (σ_c):	248	[MPa]

Specimen ID: KFM01A-113-22

Before mechanical test   After mechanical test

Diameter (mm)	Height (mm)	Density (kg/m³)
51.0	127.0	2,660

Comments   Spalling on one side of the specimen along the foliation.

Specimen ID: KFM01A−113−22

Youngs Modulus (E):	76.1	[GPa]
Poisson Ratio (ν):	0.136	[−]
Axial peak stress (σ_c):	213.3	[MPa]

Specimen ID: KFM01A-113-23

Before mechanical test   After mechanical test

Diameter (mm)	Height (mm)	Density (kg/m³)
51.1	127.0	2,650

Comments   Spalling on one side of the specimen along the foliation.

Specimen ID: KFM01A−113−23

Youngs Modulus (E):	77.9	[GPa]
Poisson Ratio (ν):	0.24	[−]
Axial peak stress (σ_c):	249.1	[MPa]
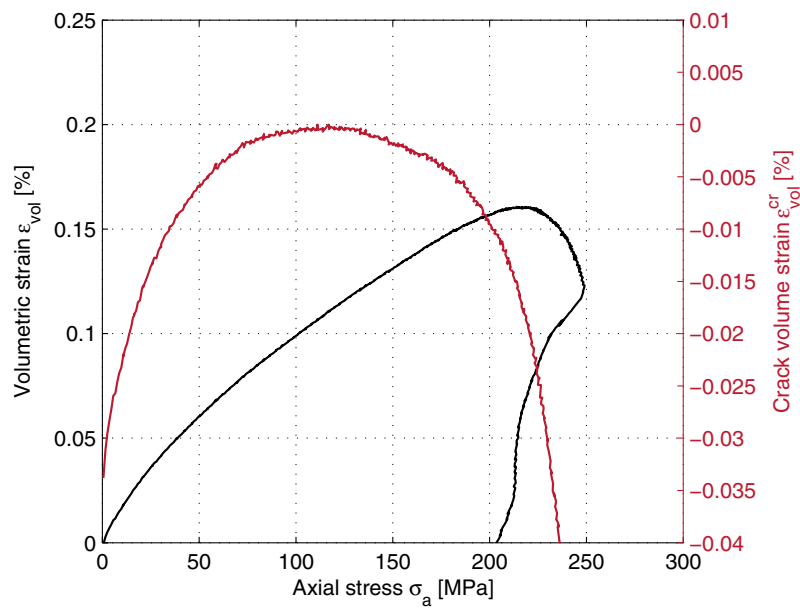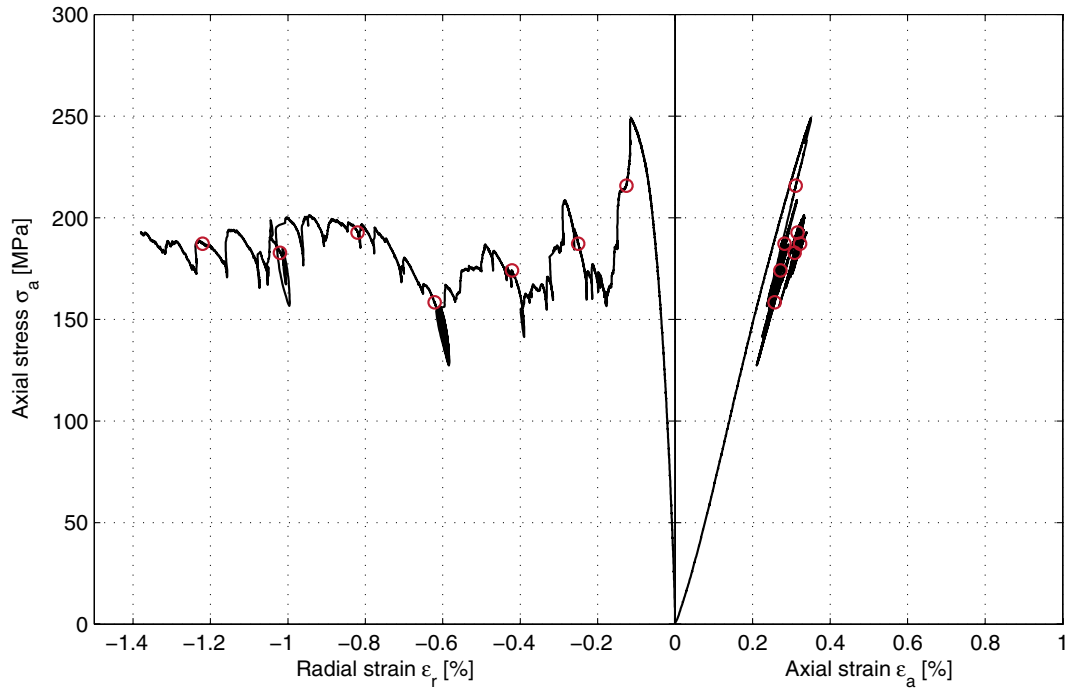
5.2   Summary of all results

A summary of the test results is shown in Tables 5-1 and 5-2. The density, uniaxial compressive strength, the tangent Young's modulus and the tangent Poisson ratio versus the depth at which the samples are taken (borehole length), are shown in Figures 5-1 to 5-4.

Table 5-1. Summary of results.

Identification	Density (kg/m³)	Compressive strength (MPa)	Young's modulus (GPa)	Poisson ratio (–)	K_{system} (MN/m)
KFM01A-113-1	2,660	270.1	81.9	0.24	8.34
KFM01A-113-2	2,660	269.7	78.1	0.21	14.97
KFM01A-113-3	2,650	220.4	79.1	0.25	11.77
KFM01A-113-4	2,660	224.1	74.0	0.22	14.36
KFM01A-113-5	2,650	227.0	79.8	0.28	7.46
KFM01A-113-8	2,660	187.4	78.9	0.24	10.00
KFM01A-113-10	2,650	229.3	76.1	0.20	11.57
KFM01A-113-12	2,660	261.6	76.5	0.22	14.47
KFM01A-113-14	2,660	238.9	74.2	0.18	16.46
KFM01A-113-16	2,660	235.6	75.3	0.23	11.54
KFM01A-113-18	2,660	288.6	78.0	0.18	12.80
KFM01A-113-20	2,660	224.6	77.8	0.27	9.58
KFM01A-113-21	2,650	248.0	76.5	0.23	10.34
KFM01A-113-22	2,660	213.3	76.1	0.14	9.49
KFM01A-113-23	2,650	249.1	77.9	0.24	7.87

Table 5-2. Calculated mean values and standard deviation.

	Density (kg/m³)	Compressive strength (MPa)	Young's modulus (GPa)	Poisson ratio (–)
Mean value	2,657	239.2	77.4	0.22
Standard deviation	4.9	25.9	2.1	0.036

Wet density
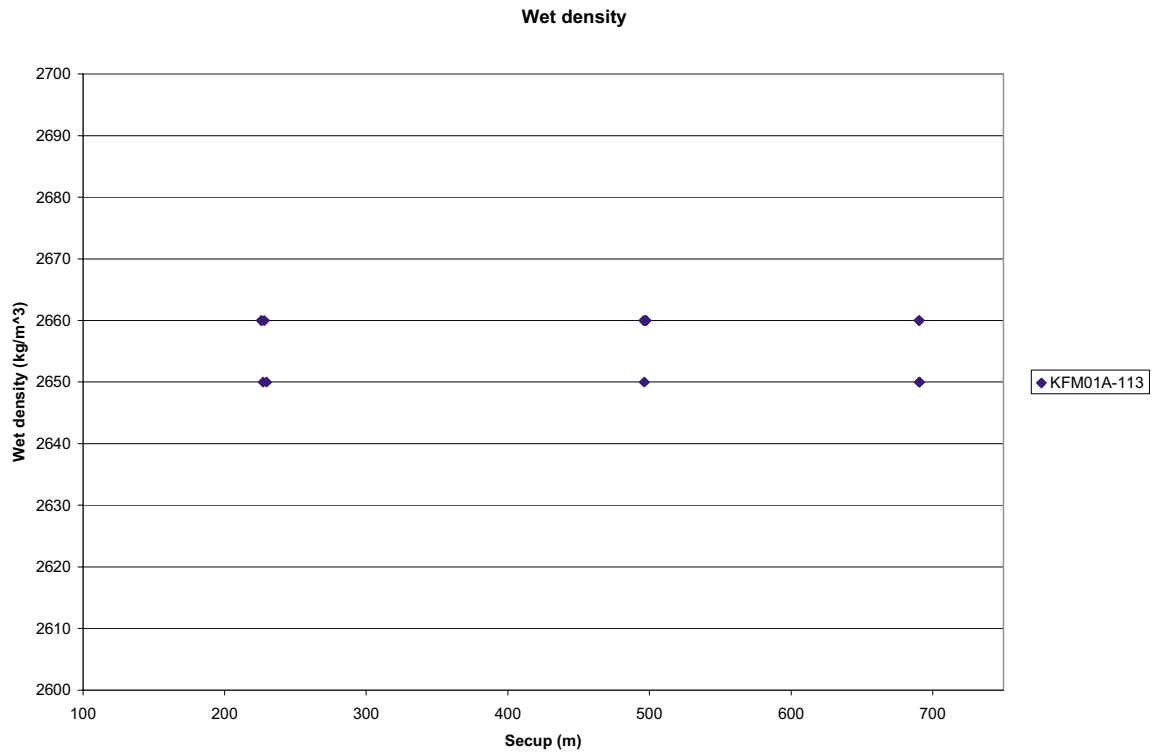
Figure 5-1. *Density versus sampling depth.*

Compressive strength
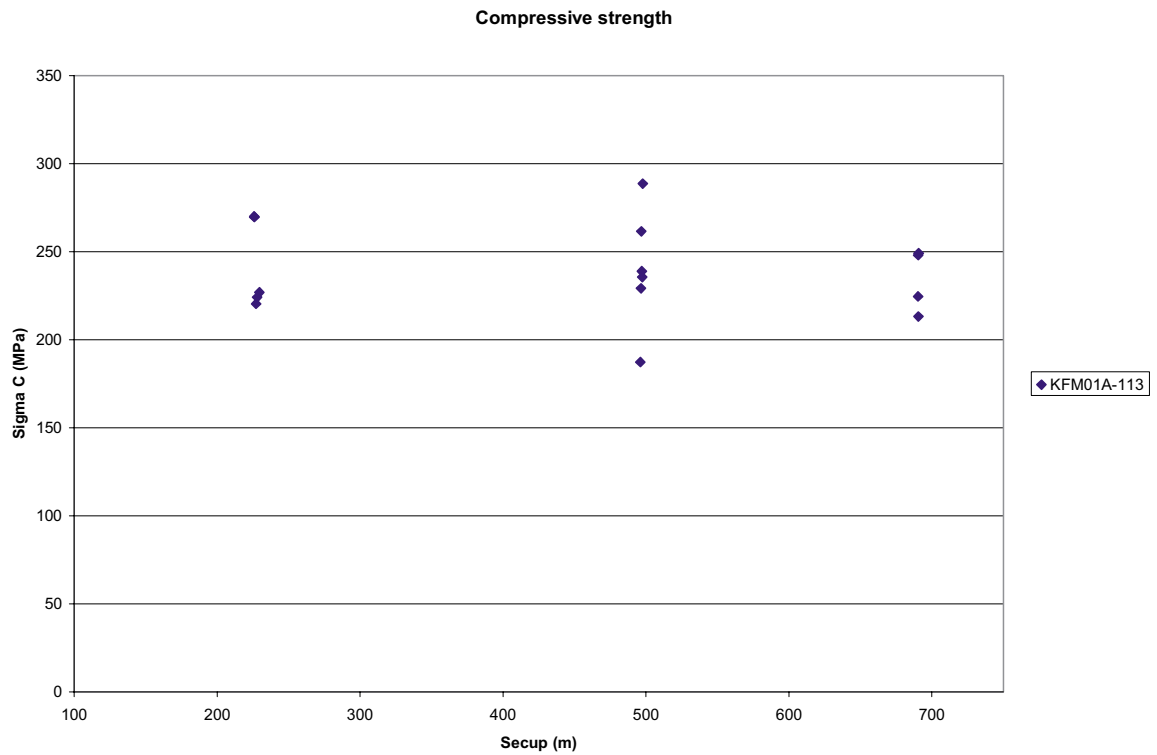
Figure 5-2. *Uniaxial compressive strength versus sampling depth.*

53
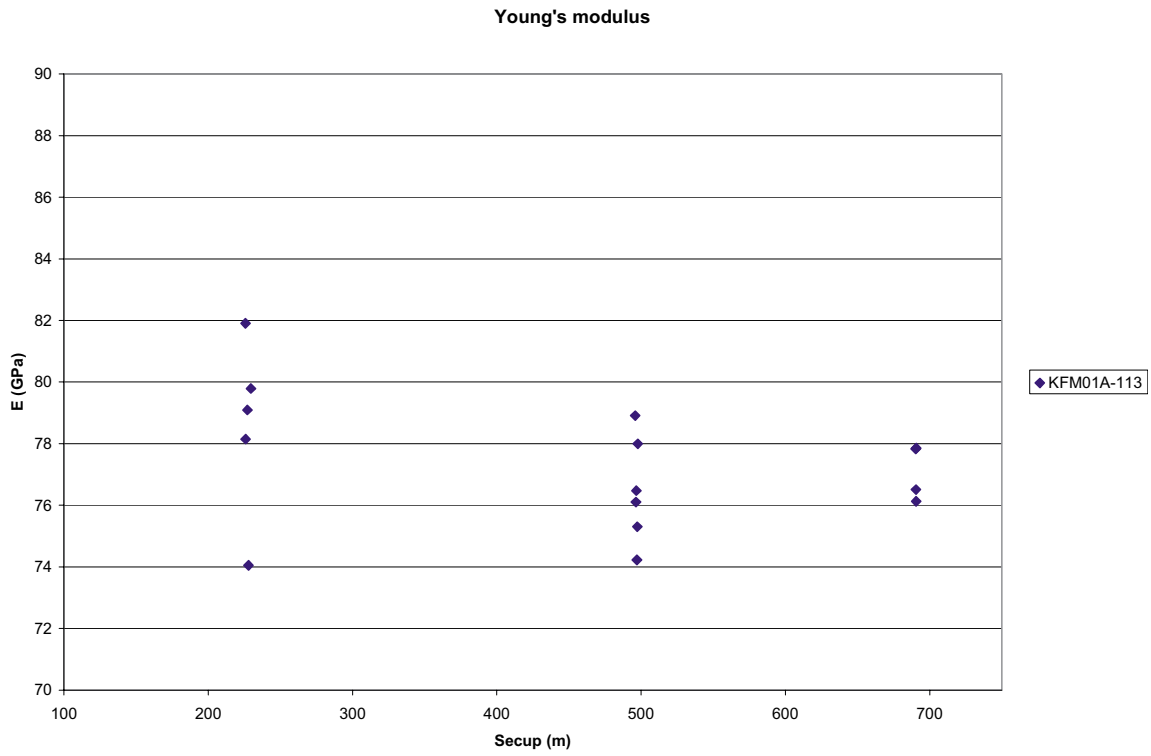
Young's modulus

Figure 5-3. *Tangent Young's modulus versus sampling depth.*
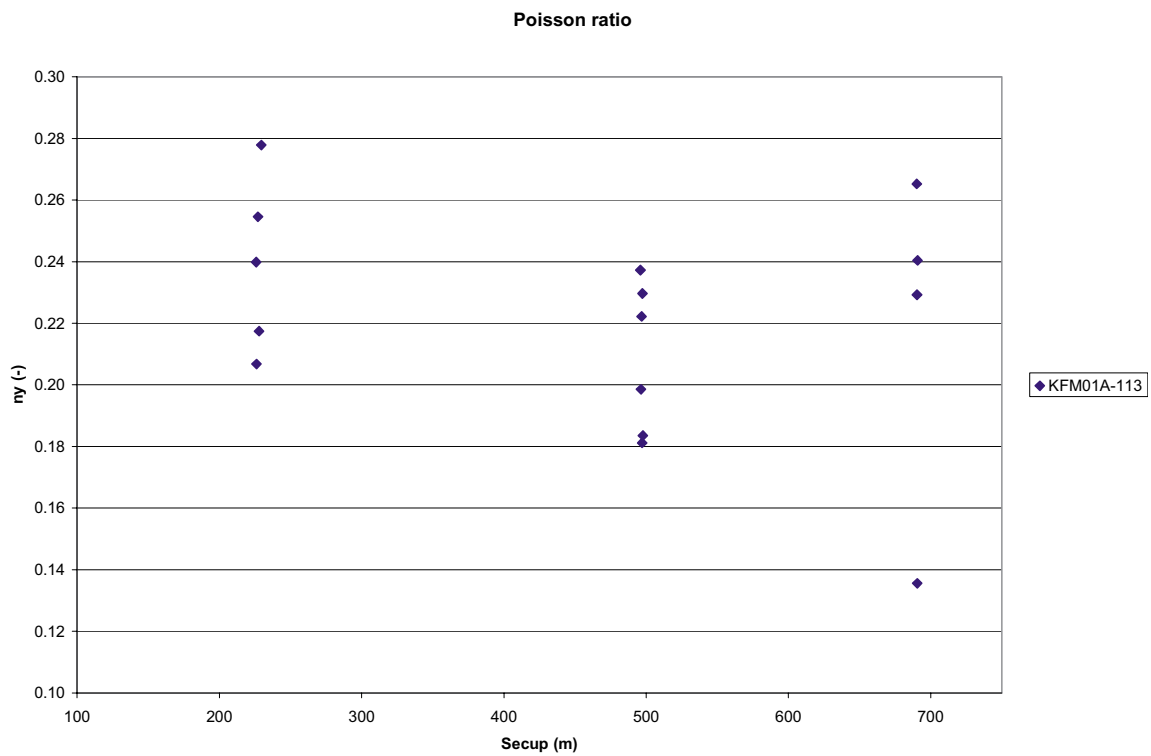
Poisson ratio

Figure 5-4. *Tangent Poisson ratio versus sampling depth.*

5.3 Nonconformities and discussion

The testing was conducted according to the method description with some deviations. The circumferential strains have been determined within a relative error of 1.5%, which is larger than what is specified in the ISRM-standard /1/. Further, double systems for measuring the axial deformation have been used, which is beyond the method description. This was conducted as a development of the test method specially aimed for high-strength brittle rock.

One test (KFM01A-113-1) was restarted after complete unloading caused by a registration of a sudden radial expansion due to cracking. This was done in order to obtain further results in the post-failure region but only in cases when the test just had entered the post failure-region and when it was judged that the specimen still had a large part of the load bearing capacity left. The radial strain feedback implies that the system responds with an unloading when an instantaneous radial expansion of the specimen takes place due to cracking.

The activity plan was followed with the exception that specimen KFM01A-113-24 was not tested, as it was defect.

References

/1/   **ISRM, 1999.** Draft ISRM suggested method for the complete stress-strain curve for intact rock in uniaxial compression. Int. J. Rock. Mech. Min. Sci. 36(3), pp. 279–289.

/2/   **Martin C D, Chandler N A, 1994.** The progressive fracture of Luc du Bonnet granite. Int. J. Rock. Mech. Min. Sci. & Geomech. Abstr. 31(6), pp. 643–659.

/3/   **Eberhardt E, Stead D, Stimpson B, Read R S, 1998.** Identifying crack initiation and propagation thresholds in brittle rock. Can. Geotech. J. 35, pp. 222–233.

/4/   **ASTM 4543-01, 2001.** Standard practice for preparing rock core specimens and determining dimensional and shape tolerance.

/5/   **ISRM, 1979.** Suggested Method for Determining Water Content, Porosity, Density, Absorption and Related Properties and Swelling and Slake-durability Index Properties. Int. J. Rock. Mech. Min. Sci. & Geomech. Abstr. 16(2), pp. 141–156.

/6/   **SS-EN 13755.** Natural stone test methods – Determination of water absorption at atmospheric pressure.

/7/   **Stråhle A, 2001.** Definition och beskrivning av parametrar för geologisk, geofysisk och bergmekanisk kartering av berg, SKB R-01-19, Svensk Kärnbränslehantering AB. In Swedish.

/8/   **MATLAB, 2002.** The Language of Technical computing. Version 6.5. MathWorks Inc.

The following equations describe the calculation of radial strains when using a circumferential deformation device, see Figure A-1.

$$\varepsilon_r = \frac{\Delta C}{C_i}$$

where

$C_i = 2 \pi R_i =$ initial specimen circumference

$\Delta C =$ change in specimen circumference $= \dfrac{\pi \cdot \Delta X}{\sin\left(\dfrac{\theta_i}{2}\right) + \left(\pi - \dfrac{\theta_i}{2}\right)\cos\left(\dfrac{\theta_i}{2}\right)}$

and

$\Delta X =$ change in LVDT reading $= X_i - X_f$
($X_i =$ initial chain gap; $X_f =$ current chain gap)

$\theta_i =$ initial chord angle $= 2\pi - \dfrac{L_c}{R_i + r}$

$L_c =$ chain length (measured from center of one end roller to center of the other end roller)

$r =$ roller radius

$R_i =$ initial specimen radius
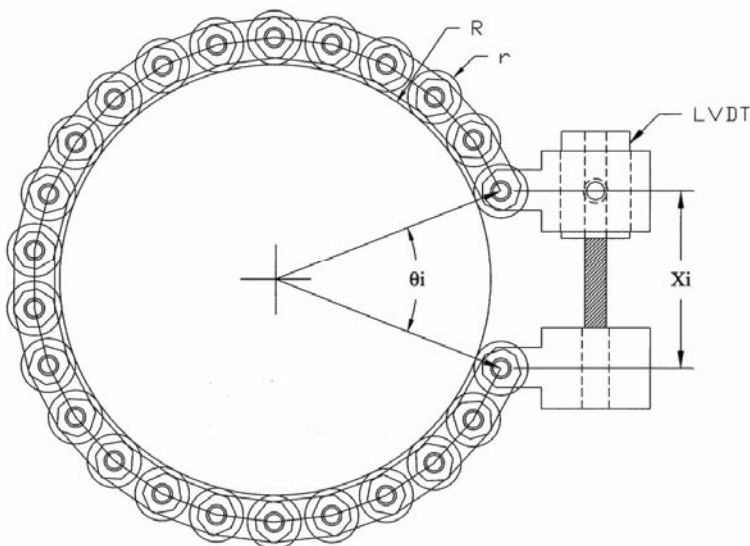
Figure A-1. *Chain for radial deformation measurement.*

This appendix contains results showing the unprocessed data and values on the computed system stiffness K_{system} that was used for the data processing, cf Section 4.4. In addition, graphs showing the volumetric strain ε_{vol} versus the axial strain ε_a and the actual radial strain rate $d\varepsilon_r$ dt versus time are displayed.

Specimen ID: KFM01A−113−01
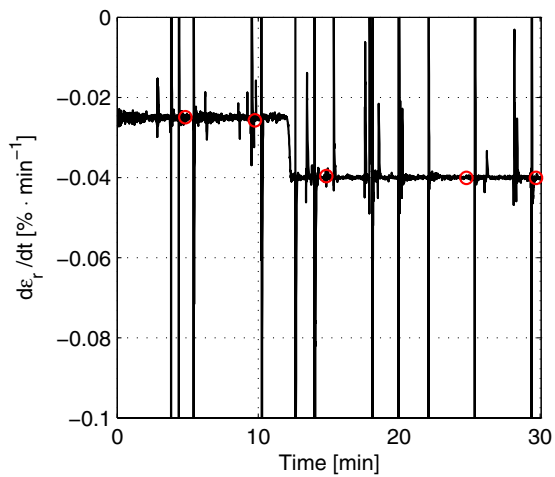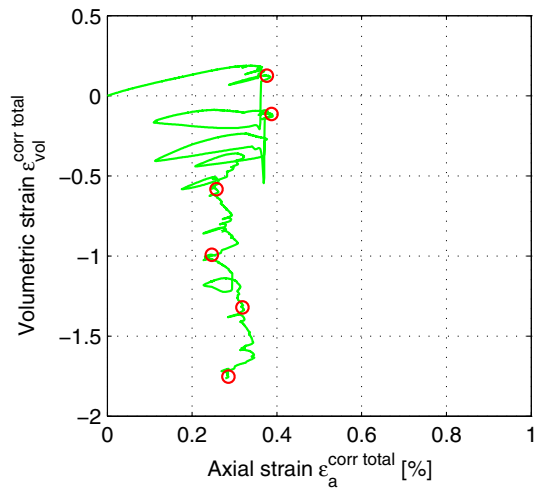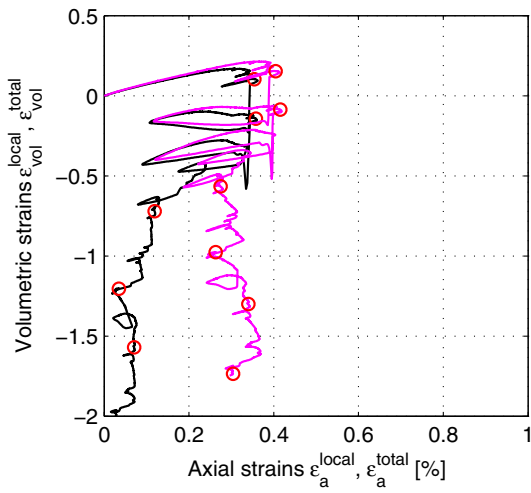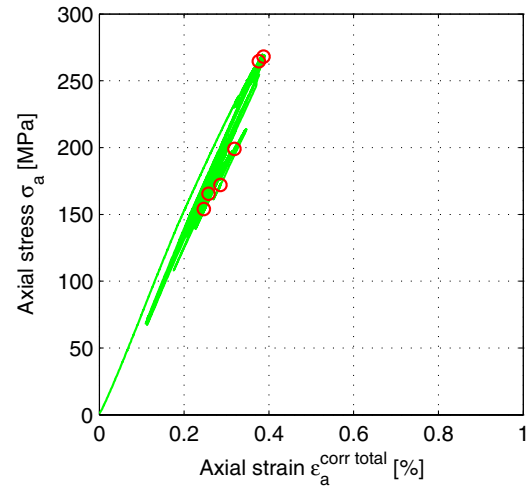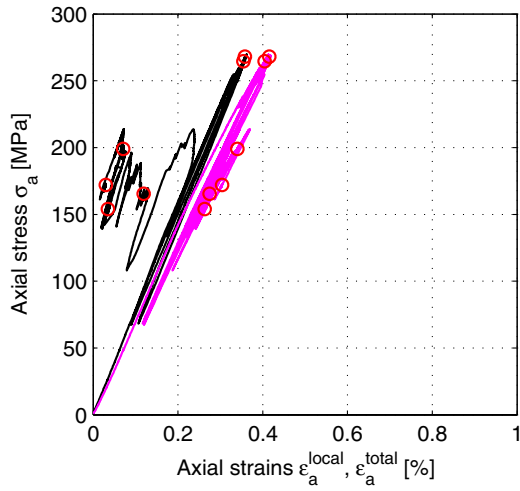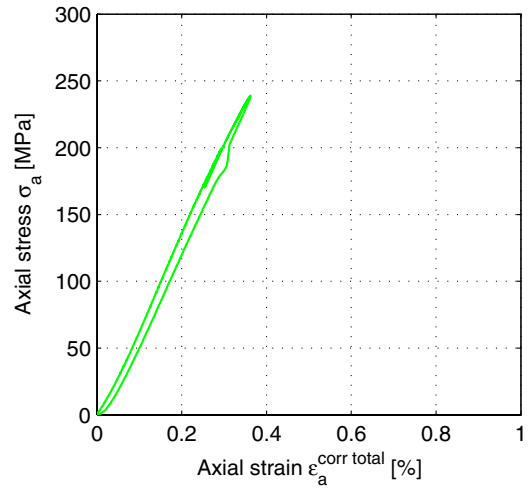

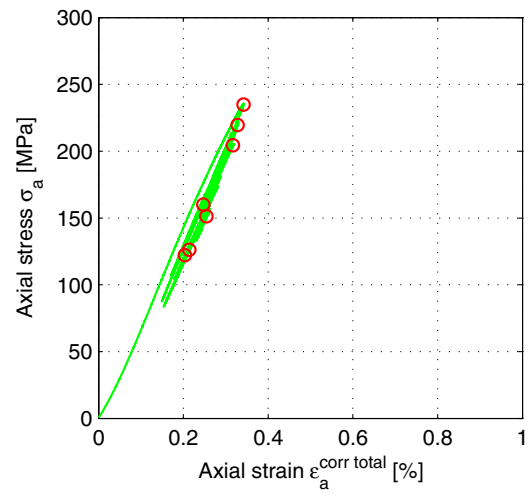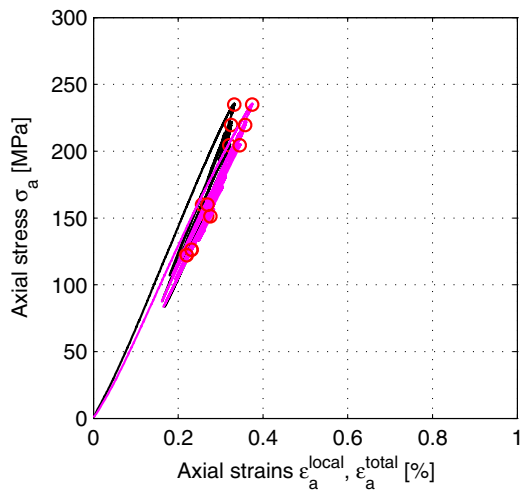Explanation to curves above:

Based on local deformation (black)

Based on total deformation (magenta)

Based on corrected deformation (green)

Calculated system stiffness:

K_{system} = 8.3435 [MN/m]

Specimen ID: KFM01A−113−02

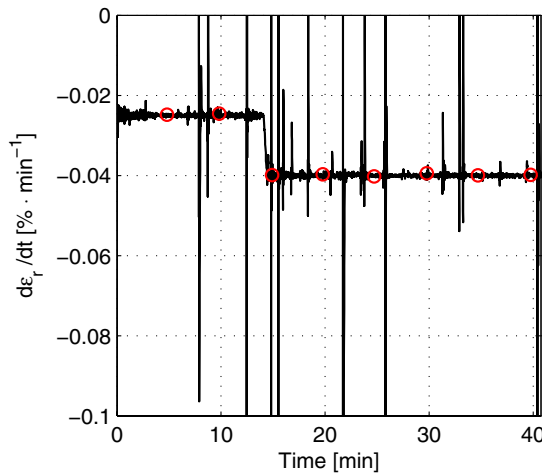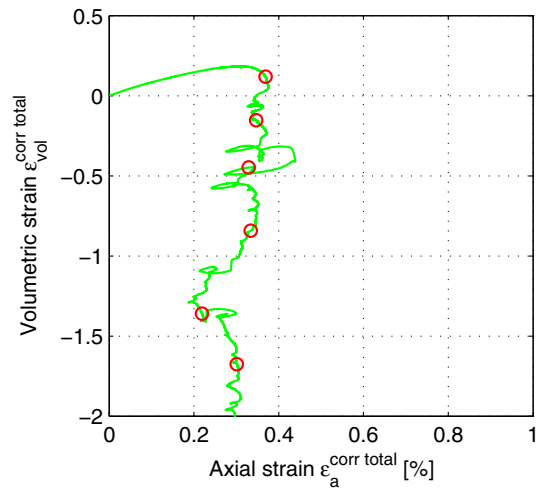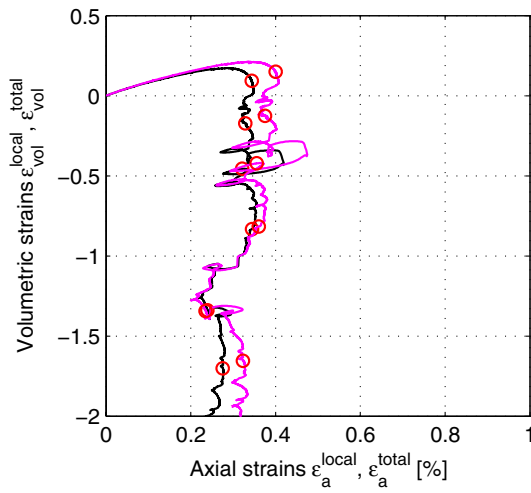Explanation to curves above:

Based on local deformation (black)

Based on total deformation (magenta)

Based on corrected deformation (green)

Calculated system stiffness:

K_{system} = 14.9673 [MN/m]

Specimen ID: KFM01A−113−03
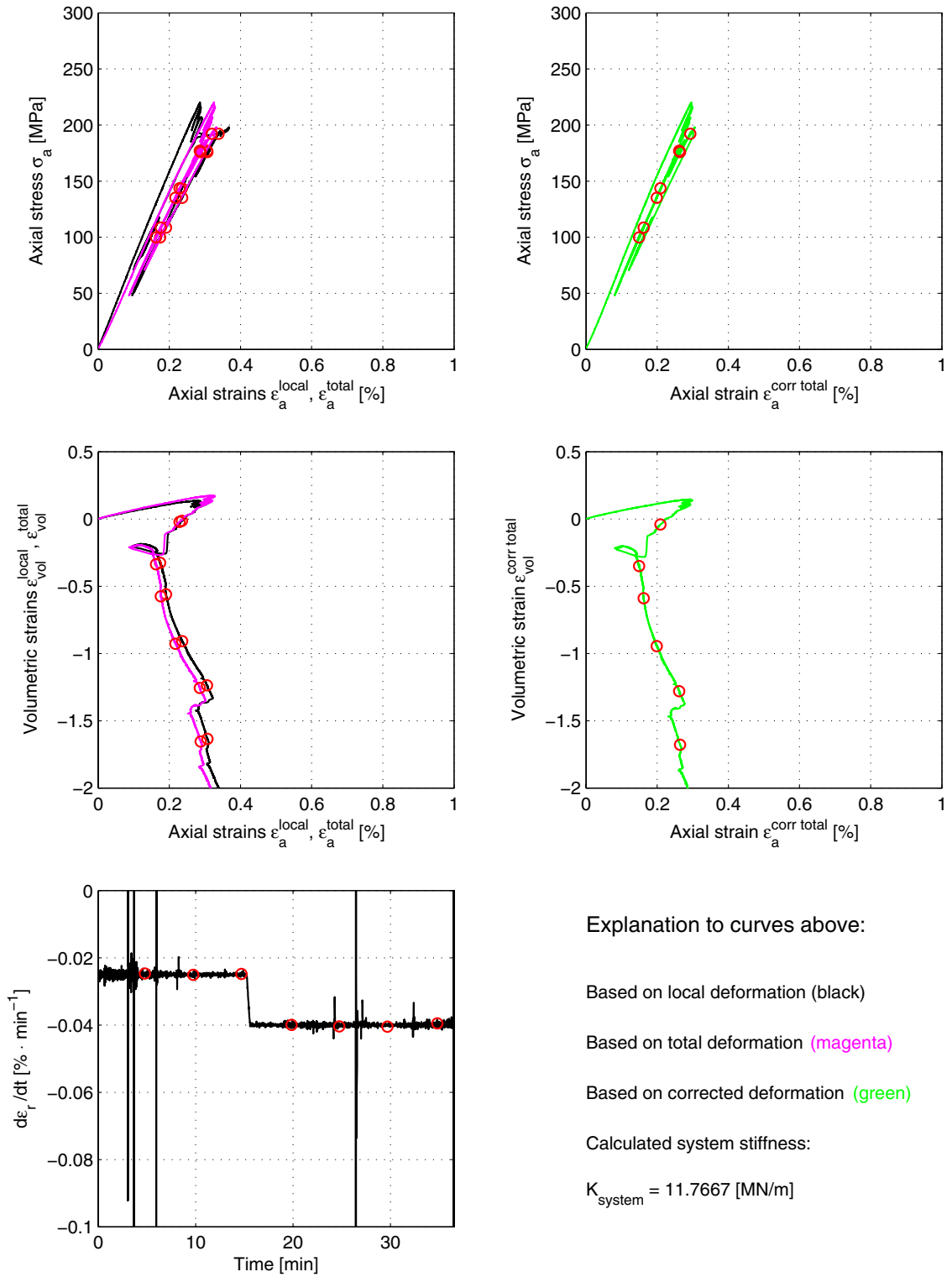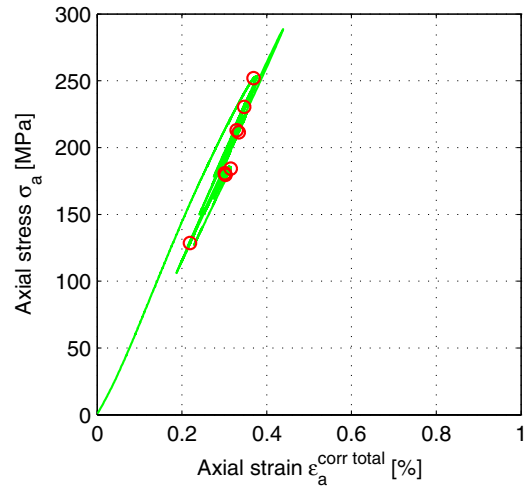

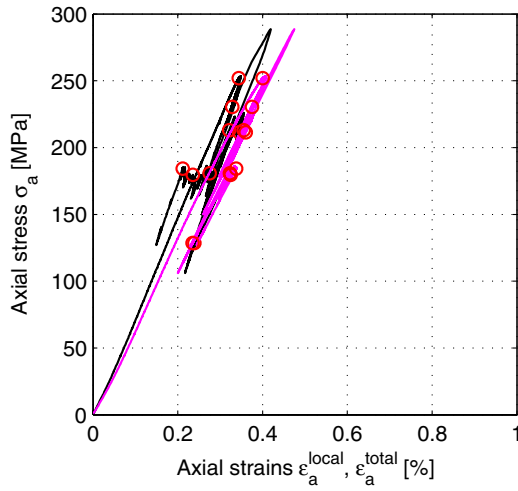Explanation to curves above:

Based on local deformation (black)

Based on total deformation (magenta)

Based on corrected deformation (green)

Calculated system stiffness:

K_{system} = 11.7667 [MN/m]

Specimen ID: KFM01A–113–04
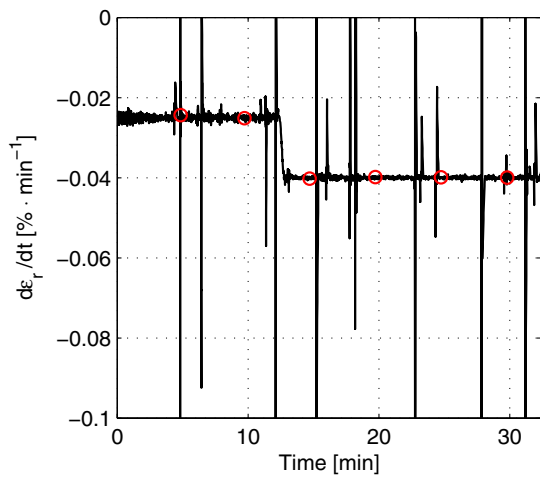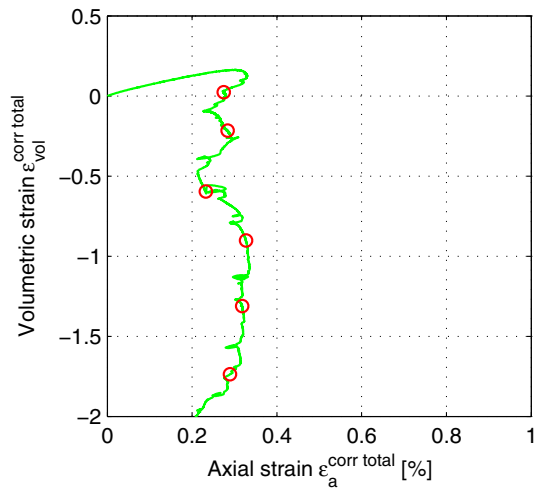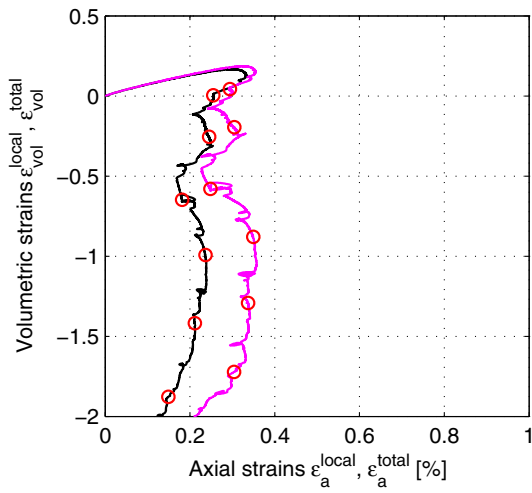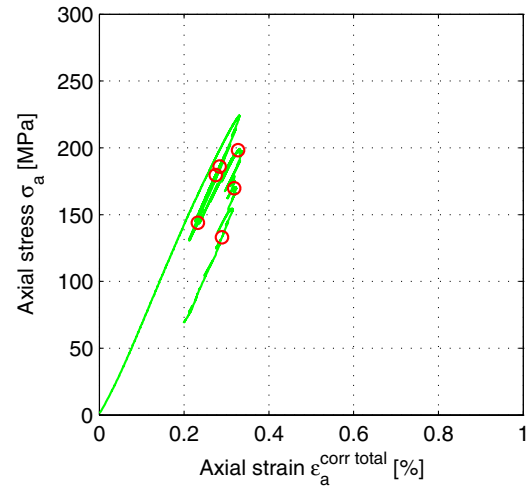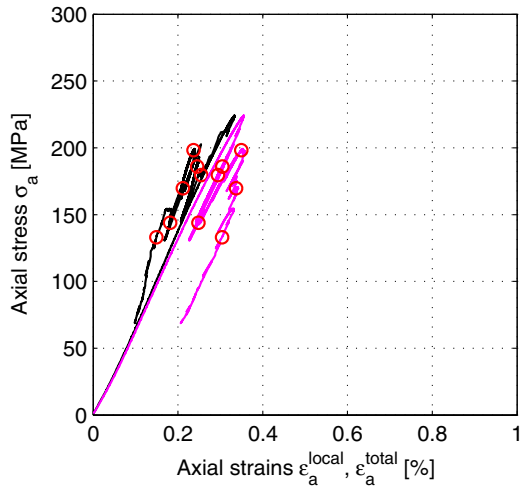
Explanation to curves above:

Based on local deformation (black)

Based on total deformation (magenta)

Based on corrected deformation (green)

Calculated system stiffness:

K_{system} = 14.3641 [MN/m]

Specimen ID: KFM01A−113−05
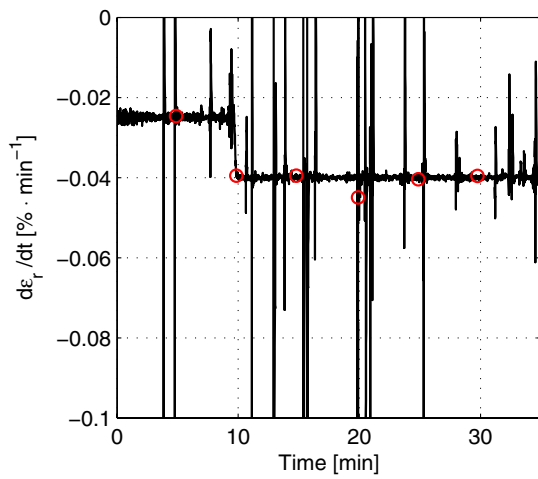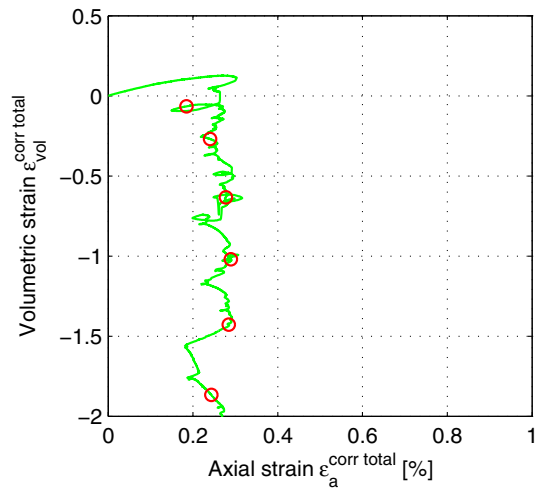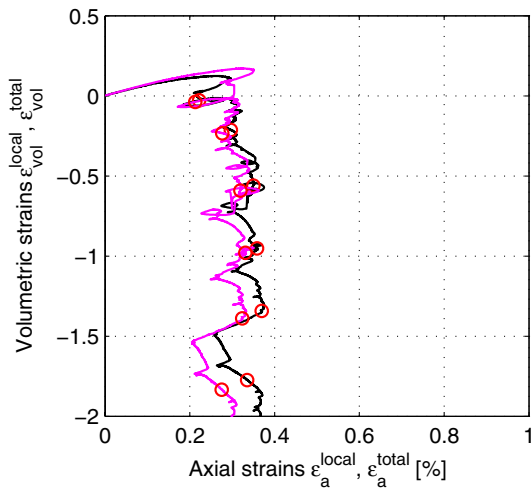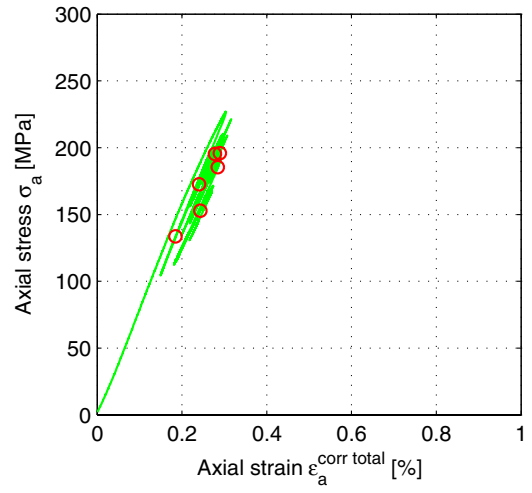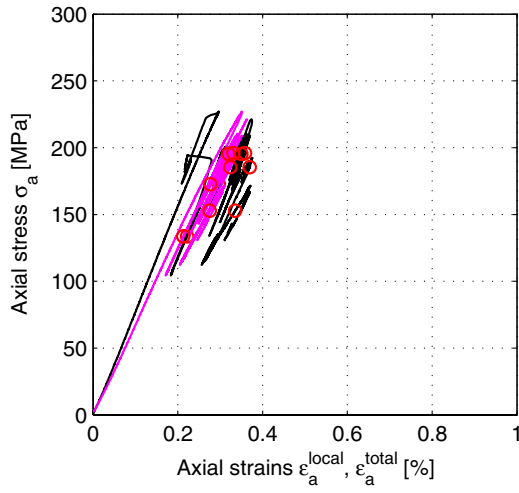
Explanation to curves above:

Based on local deformation (black)

Based on total deformation (magenta)

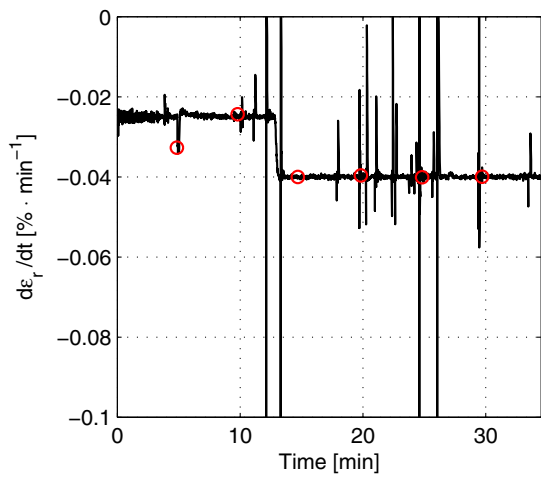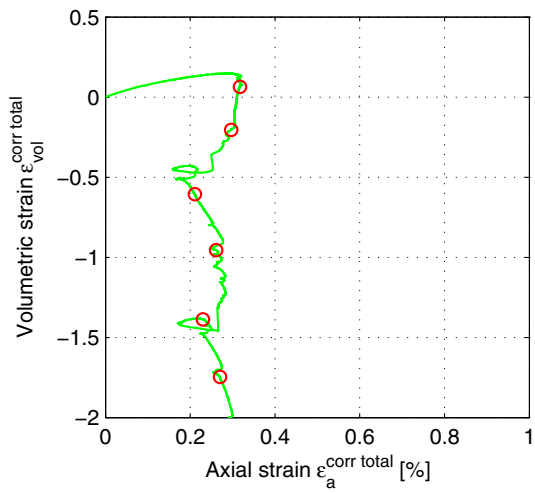Based on corrected deformation (green)

Calculated system stiffness:

$K_{system} = 7.465$ [MN/m]

Specimen ID: KFM01A−113−08
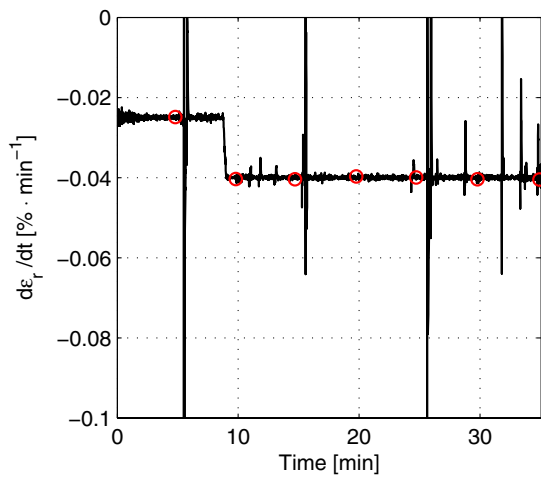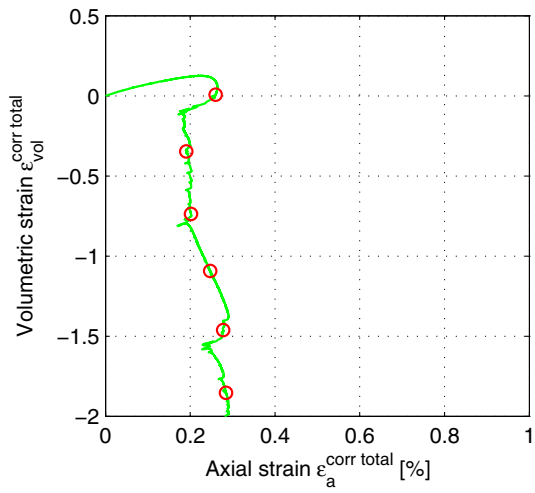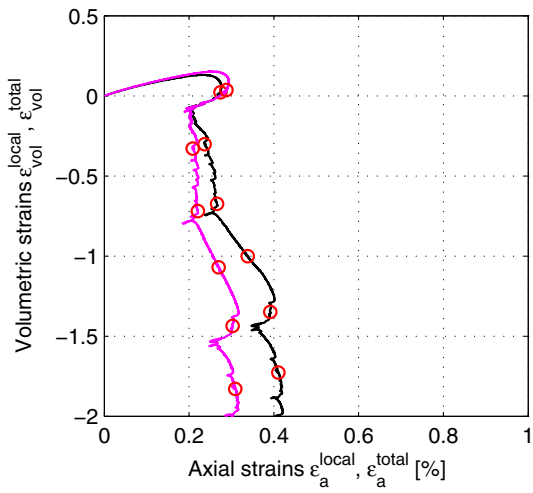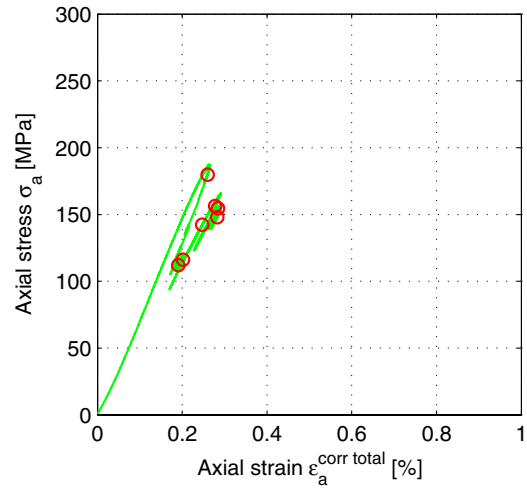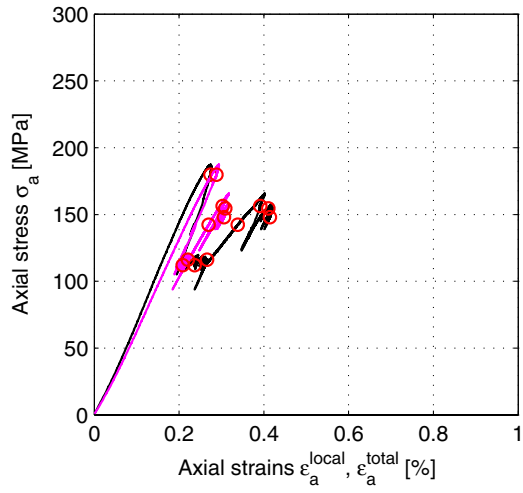
Explanation to curves above:

Based on local deformation (black)

Based on total deformation (magenta)

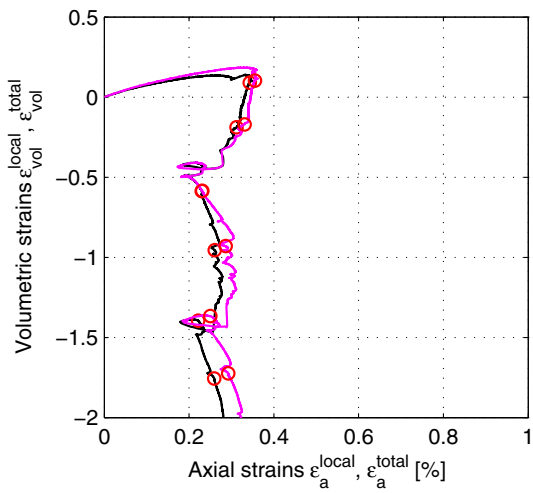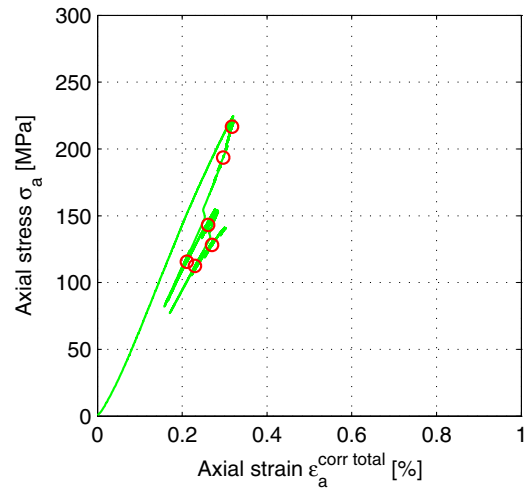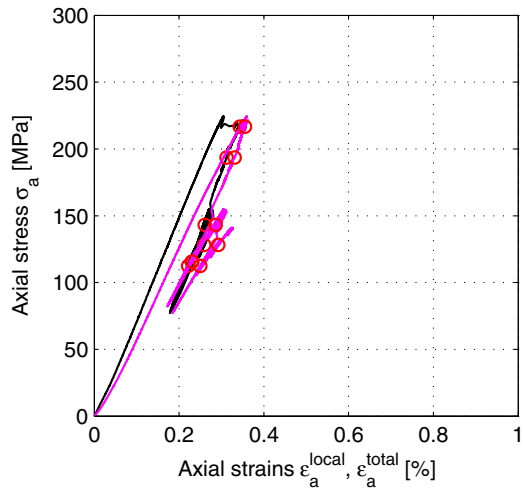Based on corrected deformation (green)

Calculated system stiffness:

K_{system} = 9.995 [MN/m]

Specimen ID: KFM01A−113−10
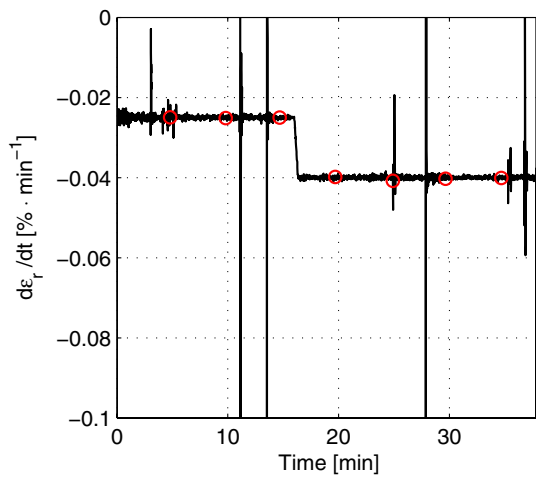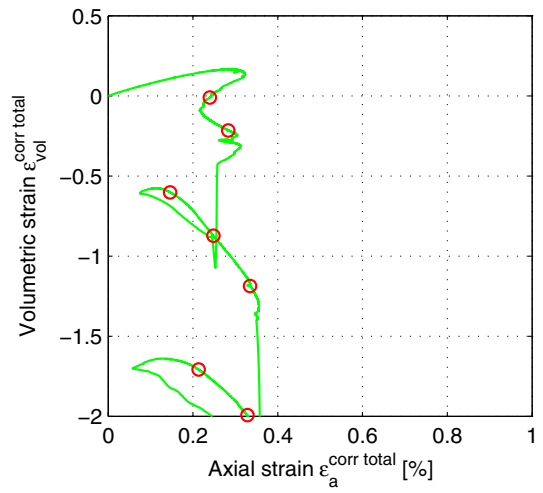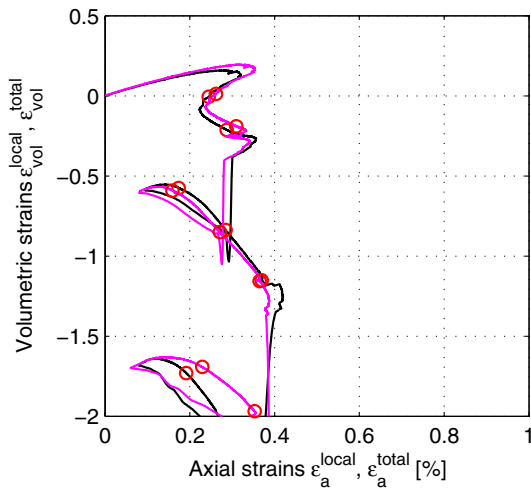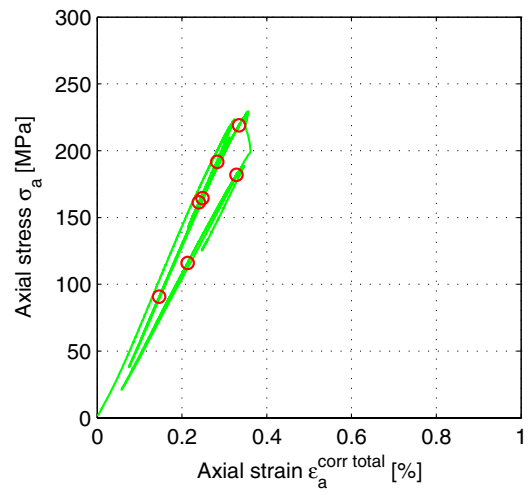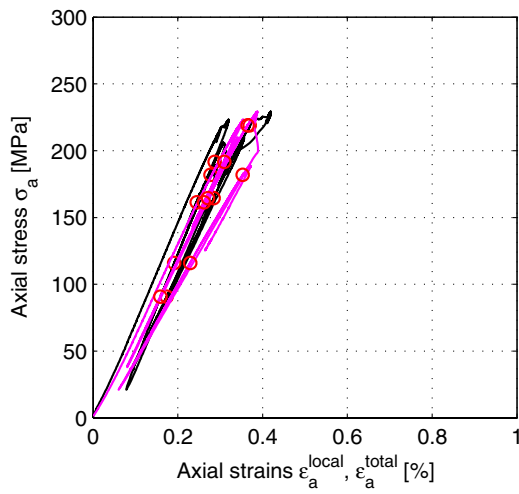
Explanation to curves above:

Based on local deformation (black)

Based on total deformation (magenta)

Based on corrected deformation (green)

Calculated system stiffness:

K_{system} = 11.5745 [MN/m]

Specimen ID: KFM01A−113−12
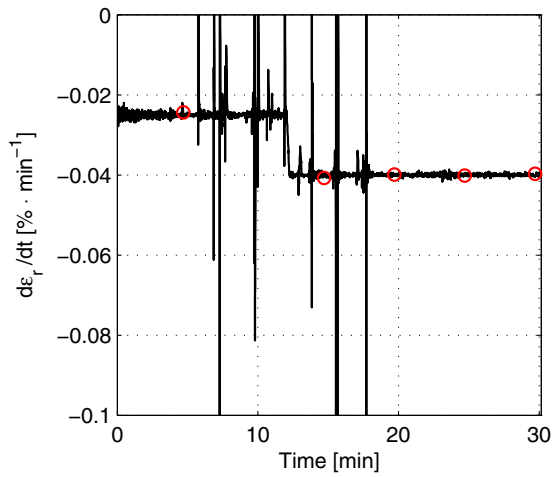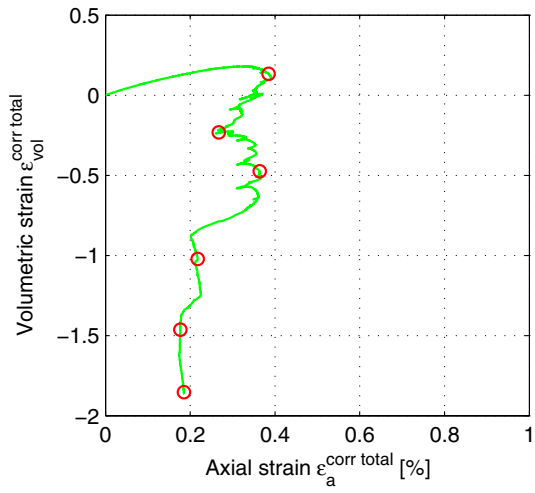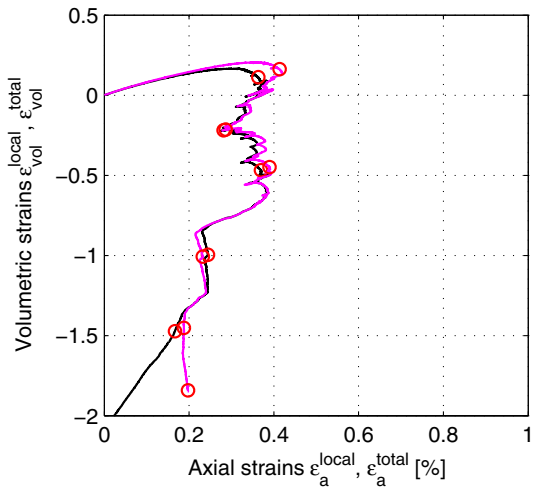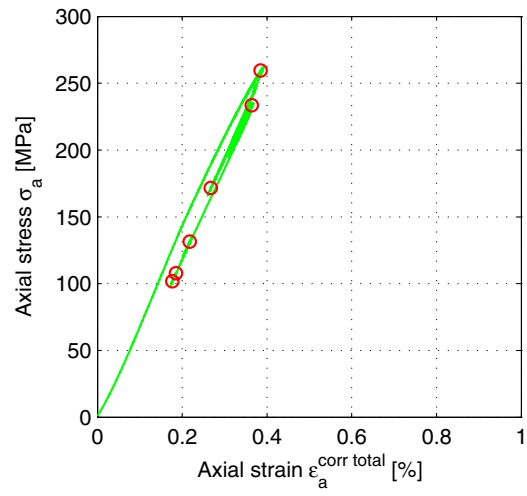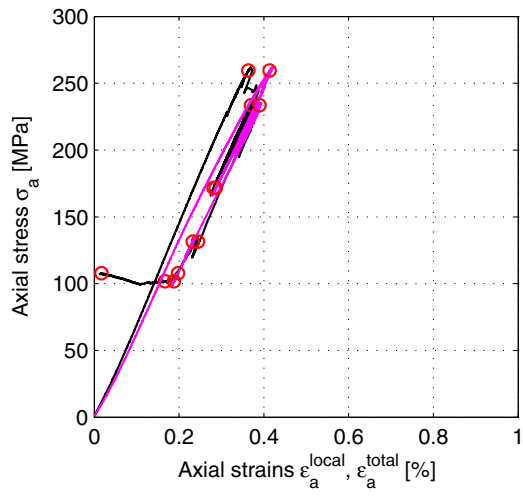
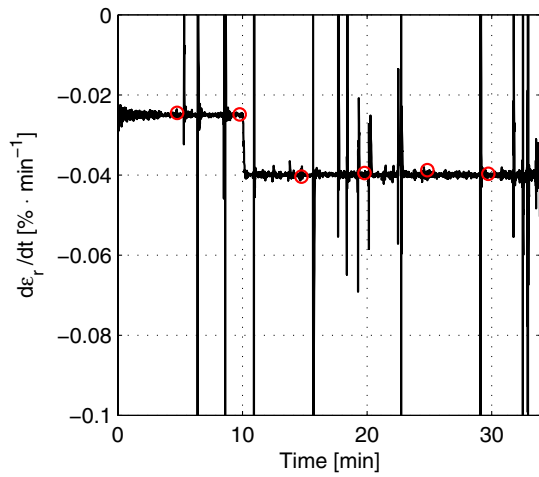Explanation to curves above:
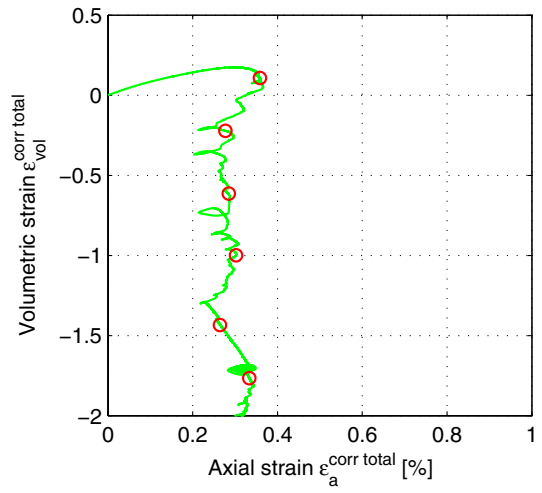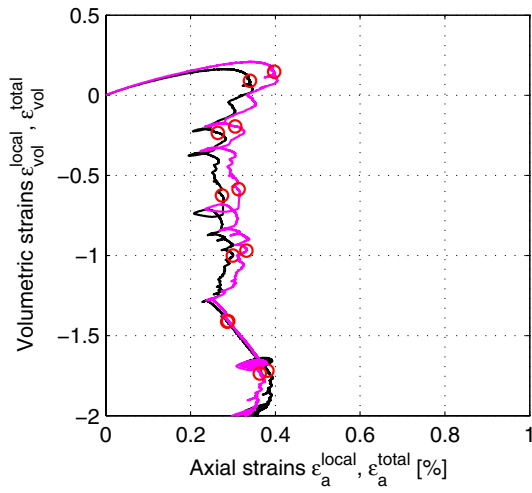
Based on local deformation (black)

Based on total deformation (magenta)

Based on corrected deformation (green)

Calculated system stiffness:

K_{system} = 14.4747 [MN/m]

Specimen ID: KFM01A–113–14
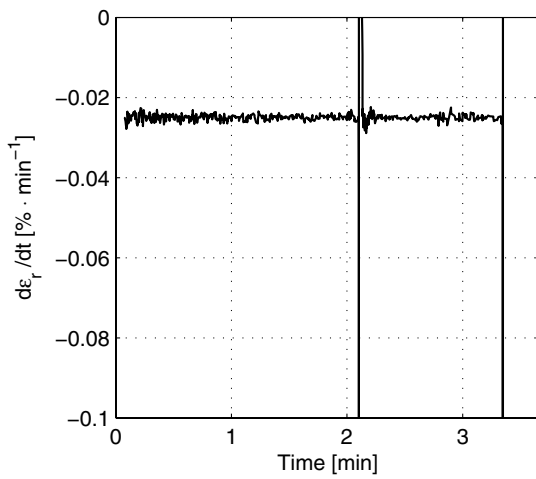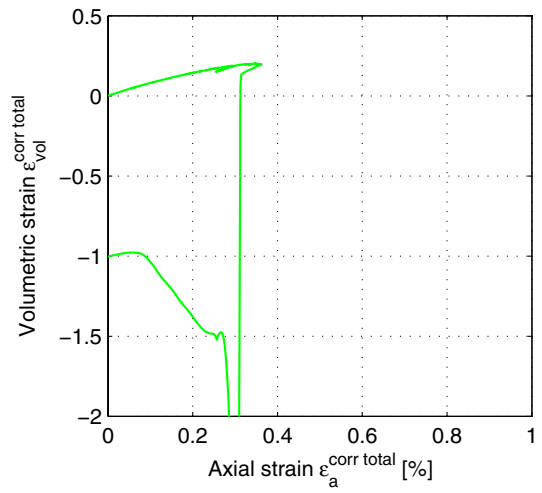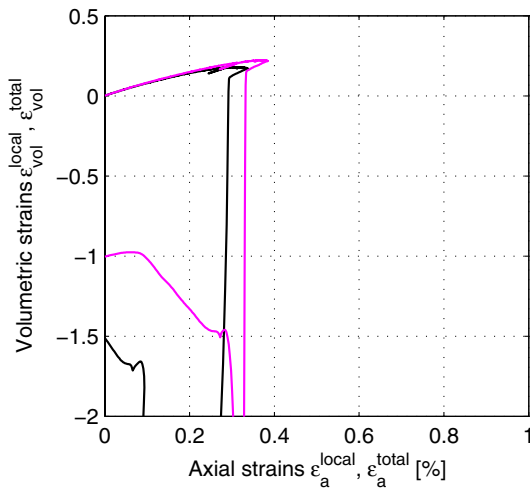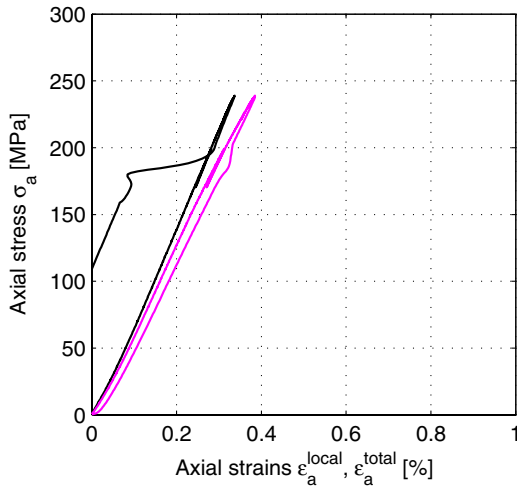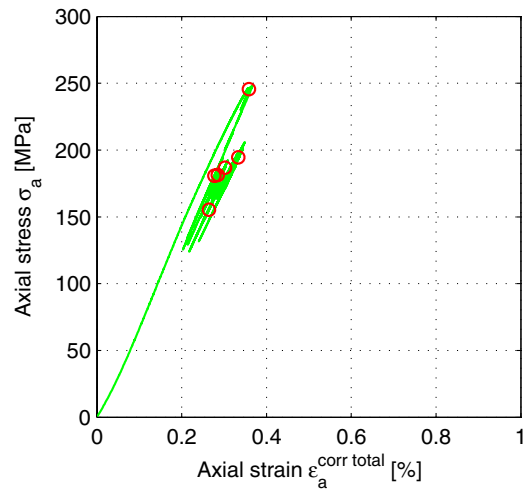

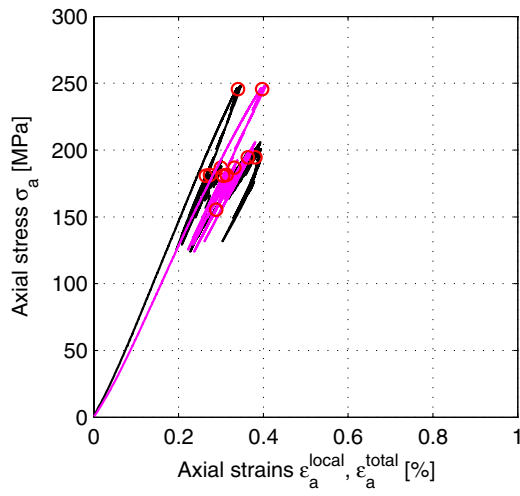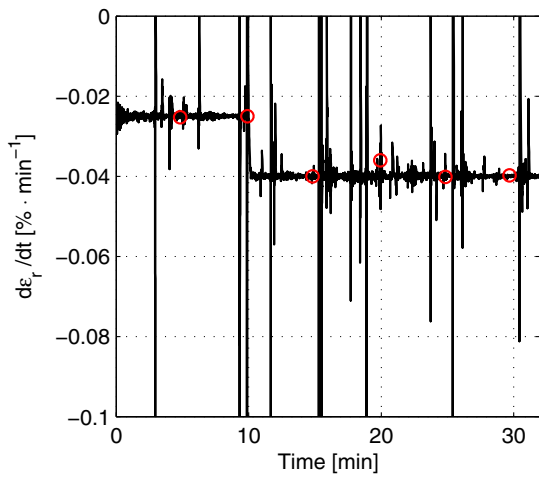Explanation to curves above:

Based on local deformation (black)

Based on total deformation (magenta)

Based on corrected deformation (green)

Calculated system stiffness:

K_{system} = 16.4563 [MN/m]

Specimen ID: KFM01A–113–16
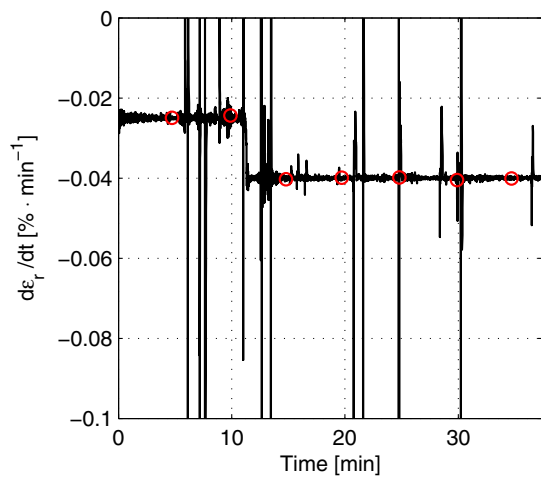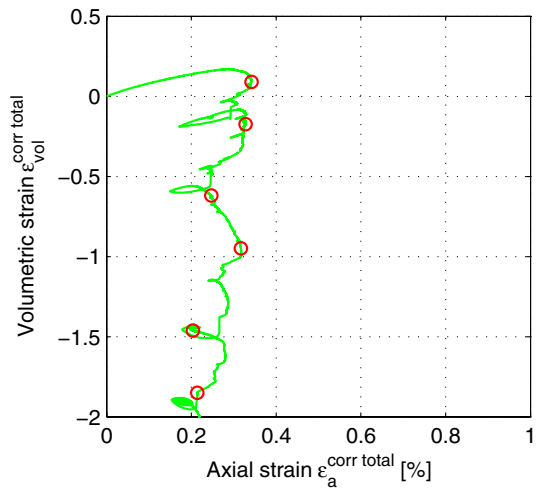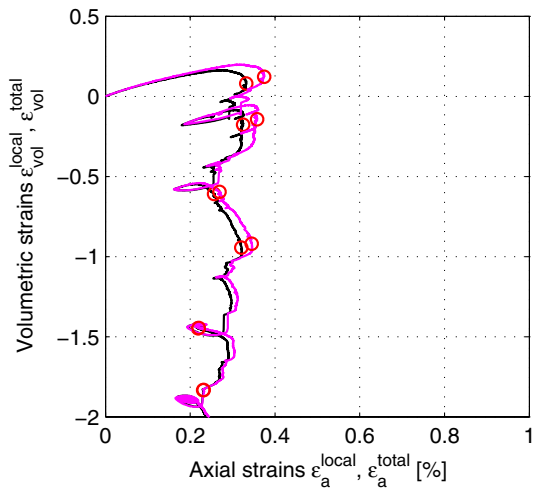
Axial stress σ_a [MPa]

Axial strains ε_a^{local}, ε_a^{total} [%]

Axial stress σ_a [MPa]

Axial strain $\varepsilon_a^{corr\ total}$ [%]

Volumetric strains $\varepsilon_{vol}^{local}$, $\varepsilon_{vol}^{total}$

Axial strains ε_a^{local}, ε_a^{total} [%]

Volumetric strain $\varepsilon_{vol}^{corr\ total}$

Axial strain $\varepsilon_a^{corr\ total}$ [%]

$d\varepsilon_r/dt$ [% · min^{-1}]

Time [min]
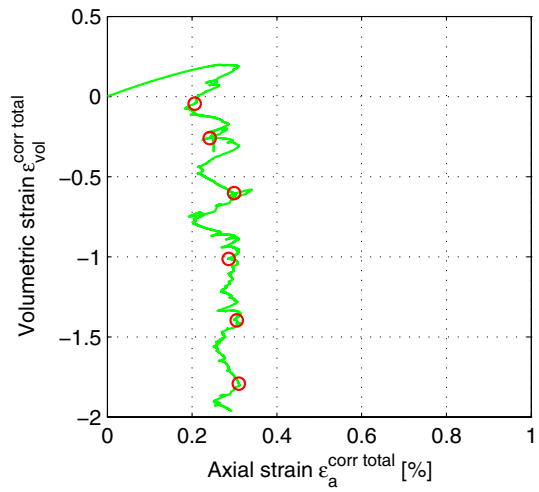
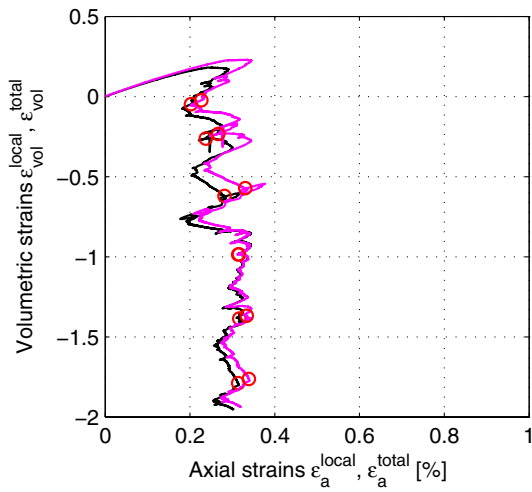Explanation to curves above:

Based on local deformation (black)

Based on total deformation (magenta)

Based on corrected deformation (green)

Calculated system stiffness:

K_{system} = 11.5382 [MN/m]

Specimen ID: KFM01A−113−18

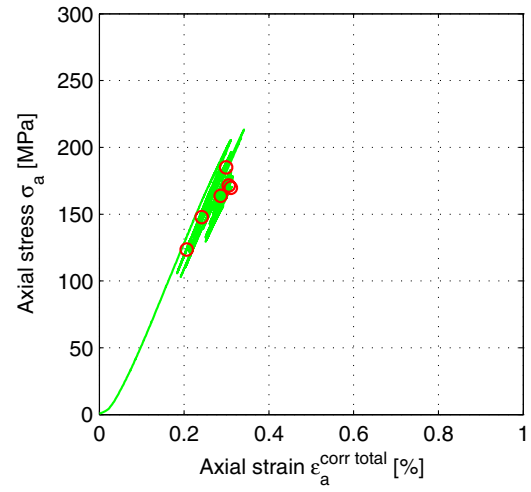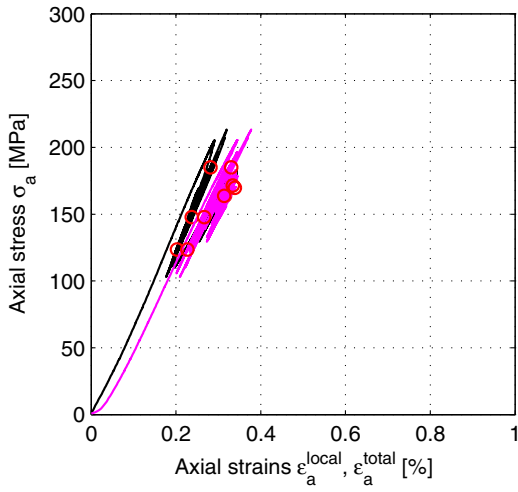Explanation to curves above:

Based on local deformation (black)

Based on total deformation (magenta)

Based on corrected deformation (green)

Calculated system stiffness:

K_{system} = 12.7999 [MN/m]

Specimen ID: KFM01A-113-20

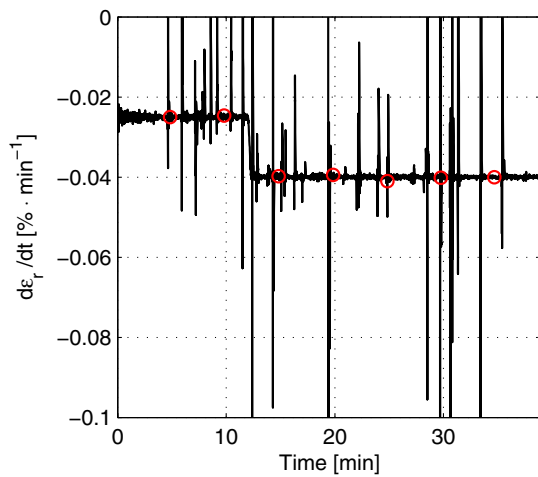Explanation to curves above:

Based on local deformation (black)

Based on total deformation (magenta)

Based on corrected deformation (green)

Calculated system stiffness:

K_{system} = 9.5782 [MN/m]

Specimen ID: KFM01A–113–21

Explanation to curves above:
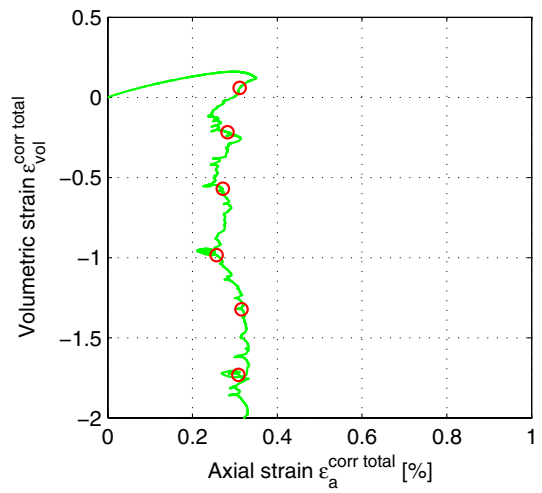
Based on local deformation (black)

Based on total deformation (magenta)

Based on corrected deformation (green)

Calculated system stiffness:

K_{system} = 10.3411 [MN/m]

73

Specimen ID: KFM01A−113−22

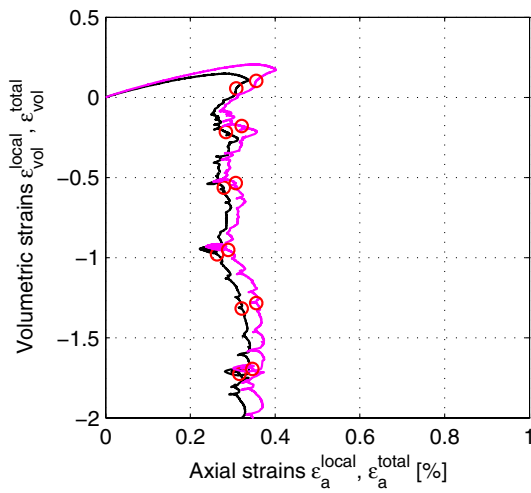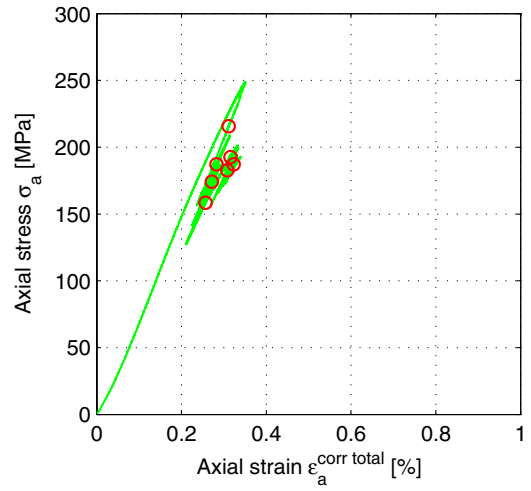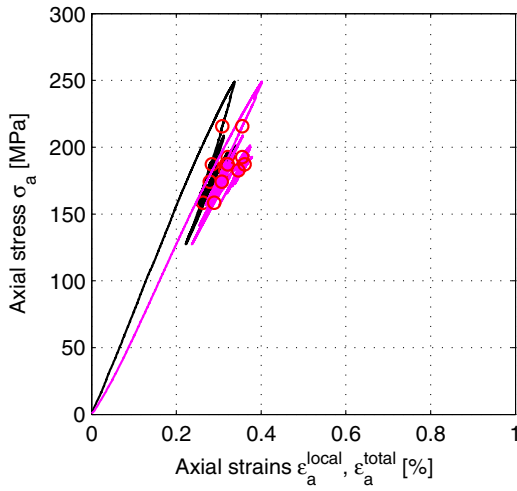Explanation to curves above:

Based on local deformation (black)

Based on total deformation (magenta)

Based on corrected deformation (green)

Calculated system stiffness:

K_{system} = 9.4883 [MN/m]

Specimen ID: KFM01A−113−23

Explanation to curves above:

Based on local deformation (black)

Based on total deformation (magenta)

Based on corrected deformation (green)

Calculated system stiffness:

K_{system} = 7.868 [MN/m]